

Learning Interpretable Differentiable Logic Networks for Time-Series Classification

Chang Yue and Niraj K. Jha

Abstract

Differentiable logic networks (DLNs) have shown promising results in tabular domains by combining accuracy, interpretability, and computational efficiency. In this work, we apply DLNs to the domain of TSC for the first time, focusing on univariate datasets. To enable DLN application in this context, we adopt feature-based representations relying on Catch22 and TSFresh, converting sequential time series into vectorized forms suitable for DLN classification. Unlike prior DLN studies that fix the training configuration and vary various settings in isolation via ablation, we integrate all such configurations into the hyperparameter search space, enabling the search process to select jointly optimal settings. We then analyze the distribution of selected configurations to better understand DLN training dynamics. We evaluate our approach on 51 publicly available univariate TSC benchmarks. The results confirm that classification DLNs maintain their core strengths in this new domain: they deliver competitive accuracy, retain low inference cost, and provide transparent, interpretable decision logic, thus aligning well with previous DLN findings in the realm of tabular classification and regression tasks.

1 Introduction

The synthesis of symbolic logic and deep learning has given rise to a new class of interpretable models that stand as a powerful alternative to opaque, black-box architectures. The pioneering work in this domain includes deep differentiable logic gate networks (LGNs) and their successor, convolutional LGNs, both proposed by Petersen *et al.* [1, 2]. These models establish a method for training networks of Boolean logic gates via gradient descent by creating differentiable relaxations of the logic operations. This core strategy yields transparent models from which logical rules can be extracted, while extensions like logical convolutions and pooling enable these architectures to scale effectively to complex classification tasks.

The LGN paradigm was significantly generalized with the development of differentiable logic networks (DLNs) [3]. By removing prior constraints, such as fixed network topologies and binary-only inputs, DLNs broadened the framework’s applicability to general tabular classification, resulting in highly efficient models that match or exceed the performance of traditional neural networks (NNs) on a wide range of benchmarks. The scope of these logic-based systems was expanded once more to handle continuous targets through the regression DLN [4]. This extension integrates a weighted sum of the final layer’s logical rule outputs to produce a numerical prediction, successfully adapting the architecture to regression while maintaining its inherent interpretability.

Despite the success of DLNs in tabular classification and their extension to regression, their application to time series data, particularly for classification tasks, remains largely unexplored. This article addresses this gap by applying the classification DLN paradigm to univariate time-series classification

Chang Yue and Niraj K. Jha are with the Department of Electrical and Computer Engineering, Princeton University, Princeton, NJ 08544, USA, e-mail: {cyue, jha}@princeton.edu.

This work was supported by the U.S. National Science Foundation under Grant CCF-2416541.

(TSC). A simplified time-series classification DLN (TSC-DLN) is shown in Fig. 1. Time-series data present unique challenges due to their sequential nature and varying lengths. This is not directly compatible with DLNs that typically require fixed-size input vectors. To overcome this obstacle, we leverage feature-based transformations that convert raw univariate time-series sequences into fixed-length feature vectors, making them suitable for DLN processing.

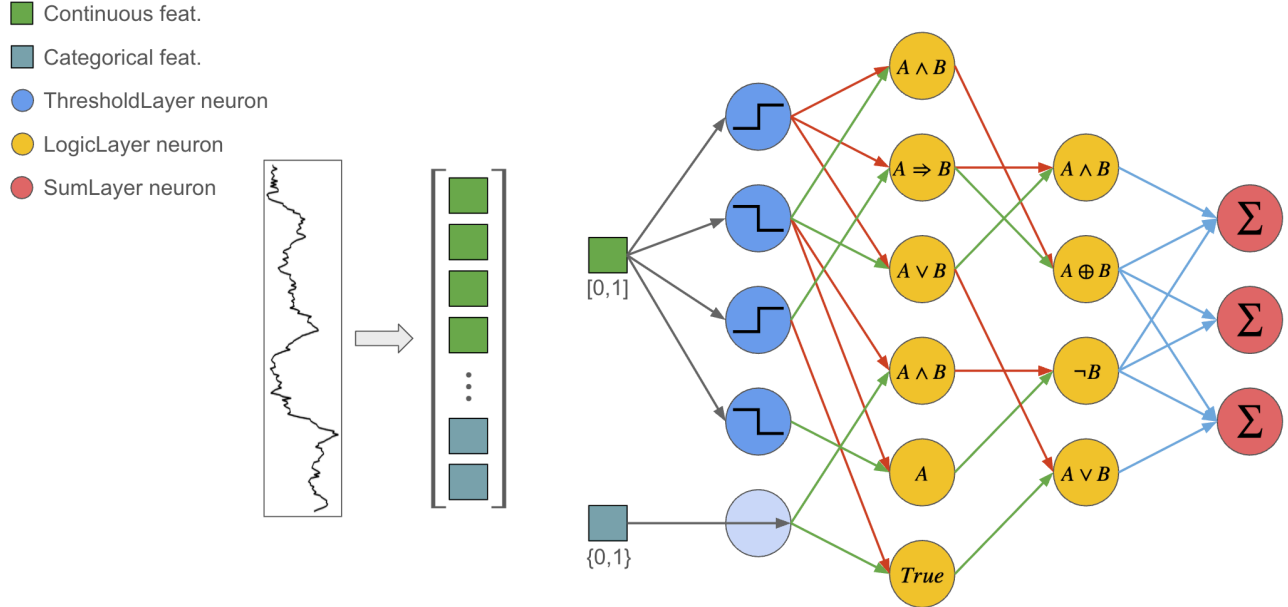


Figure 1: A simplified TSC-DLN example. First, input sequences are transformed into fixed-length vectors with values in $[0, 1]$ using candidate transformations. Then, a standard classification DLN is employed: The ThresholdLayer binarizes the continuous inputs, the LogicLayers apply binary two-input logic operations to the binarized inputs, and the SumLayer sums the scores for each class.

Specifically, we employ two distinct feature extraction methodologies: Catch22 [5] and TSFresh [6]. *Catch22* (CAnonical Time-series CHaracteristics) includes distillation of approximately 7700 candidate statistics extracted from the extensive *hctsa* [7] repository into a fixed compact set of 22 carefully chosen, non-redundant features. These features are not only interpretable and fast to compute but also collectively cover a wide range of time-series concepts, offering strong classification accuracy across diverse benchmarks. The second method, *TSFresh* (Time Series FeatuRe Extraction on basis of Scalable Hypothesis tests), is a comprehensive library capable of automatically extracting nearly 800 time-series features using 63 different characterization methods. In our experiments, to manage the high dimensionality of TSFresh, we employ cross-validated random forests to select smaller feature subsets of sizes 10, 20, or 40 for each dataset. This strategy serves two primary purposes. First, it significantly reduces the input dimension and lowers computational costs and, second, provides a more direct comparison with the 22 features extracted using Catch22. Crucially, both Catch22 and TSFresh extract a fixed number of features, independent of the original time-series sequence length. This is essential for the application of classification DLNs and other methods that require a predefined input size.

Another significant contribution of this work is an integrated study of DLN training configurations. Prior DLN studies typically adopted a fixed training setting and conducted ablation studies by altering one flag at a time. For instance, the original DLN work found that learning neuron operations and connections separately yielded better average balanced accuracy across 20 classification datasets, whereas the study on the regression DLN found that learning them simultaneously resulted in a better average R^2 score. In contrast, our approach integrates various DLN training settings, such as the use of

straight-through estimators (STEs), the number of candidate logic gate and input link options for each logic operator, and whether to train neuron functionalities and connections simultaneously, into a comprehensive hyperparameter search space. We then allow a search algorithm to determine the optimal configuration, followed by a detailed statistical analysis of the settings chosen by the hyperparameter optimization (HPO) process.

To rigorously evaluate our proposed methodology and the impact of training configurations, we conduct extensive DLN experiments on 51 univariate TSC datasets from the UCR benchmark suite [8], testing a total of four transformation methods (Catch22; TSFresh with its three feature subsets). We further compare the performance of our DLN approach against both traditional machine learning methods and state-of-the-art neural networks, demonstrating its efficacy and interpretability in the time-series domain.

The remainder of this article is organized as follows. Section 2 provides an overview of related work on interpretable logic networks and time-series tasks. Section 3 details the classification DLN architecture and the feature transformation pipelines. Section 4 presents the experimental setup, results, and a comprehensive analysis of the DLN training configurations. Finally, Section 5 concludes the article with a summary of findings and outlines directions for future research.

2 Related Work

This research builds upon the previously developed DLN framework and enhances it to the domain of TSC. We first summarize the core principles of DLNs and then review related work on time-series analysis.

2.1 The Differentiable Logic Network Framework

DLN is a neuro-symbolic architecture introduced for tabular classification [3] and later extended to regression [4]. DLN design is guided by three fundamental principles:

- **Differentiability:** The differentiability of the DLN framework is founded on the combination of real-valued logic and softmax function. Real-valued (or fuzzy) logic [9, 10] enables use of the continuous domain for the operations themselves. The softmax function then serves as a differentiable proxy for ‘choose-one-from- N ’ structural decisions, such as selecting a specific logic gate or input connection.
- **Interpretability:** DLNs are inherently interpretable, producing a final model that is a clear, human-readable logical formula. This intrinsic transparency removes the need for potentially unreliable post-hoc explainers, such as LIME (Local Interpretable Model-Agnostic Explanations) or SHAP (Shapley Additive Explanations) that are applied to black-box models [11–13]. The goal is to create a model that is transparent by design, aligning with other interpretable systems like decision trees and rule-based models [14–16].
- **Efficiency:** The architecture is inherently efficient. The learning process promotes sparsity, resulting in a lightweight final model. Because the model is composed of simple operations, it is computationally fast at inference time and well-suited for deployment on resource-constrained hardware or accelerators like FPGAs, which excel at running binarized and logic-based networks [2, 17].

In this article, we demonstrate the versatility of an enhanced DLN framework by applying it to TSC, achieved by integrating a time-series feature transformation front-end.

2.2 Time-series Classification

Time-series data, i.e., sequences of observations ordered chronologically, are ubiquitous across many domains, including finance, healthcare, and industrial monitoring. Analysis of such data encompasses a variety of tasks, such as forecasting future values, clustering similar series, detecting anomalies, and classification. These tasks may involve either univariate time series, which consist of a single sequence of observations, or multivariate time series, which involve multiple time-dependent variables. To standardize the evaluation of algorithms for these tasks, several benchmark archives have been developed, with the UCR/UEA Time-Series Classification Archive being one of the most widely used and recognized [8, 18].

The field of TSC has seen a significant expansion with diverse methodologies. A comprehensive review and experimental evaluation by Bagnall *et al.* [19] organizes the landscape of TSC algorithms into eight distinct families. These families include: 1) Distance-based methods that classify series based on their proximity under a specific distance measure, with dynamic time warping being a classic example [20]; 2) Feature-based methods that transform the series into a vector of summary statistics [5, 6, 21]; 3) Interval-based approaches that extract ensembles of features from various intervals, such as QUANT [22]; 4) Shapelet-based methods that identify discriminative sub-sequences (shapelets) to distinguish between classes [23]; 5) Dictionary-based methods, where histograms of counts of repeating patterns serve as features for a classifier, exemplified by BOSS [24] and symbolic Fourier approximation [25]; 6) Convolution-based approaches that use convolutional kernels to detect patterns [26]; 7) Deep learning models that leverage neural networks [27, 28]; and 8) Hybrid approaches that combine two or more of these families [29].

Our work focuses on feature-based methods that transform a time series of arbitrary length into a fixed-length feature vector, enabling the use of standard machine learning classifiers. This approach offers an interpretable way to handle time-series data. Prominent examples of feature-based toolkits include *Catch22* [5] that provides a curated set of 22 highly informative and minimally redundant features, and *TSPresh* [6] that extracts a comprehensive set of over 750 features. While our primary focus is on these feature extraction libraries, it is worth noting that other transformation techniques also convert sequences into a vector format. For instance, the random dilated shapelet transform [30] uses an efficient transformation based on randomly generated, dilated subsequences (shapelets). Similarly, the dictionary-based WEASEL 2.0 [31] and the convolution-based ROCKET [32] frameworks also produce feature vectors from the original time series, demonstrating the convergence of different algorithmic families towards a transformation-based paradigm.

Many of the aforementioned techniques were initially developed for univariate time series. Extending them to the multivariate domain is an active area of research. Broadly, these extensions can be categorized into channel-independent and cross-channel approaches. Channel-independent methods, such as the collective of transformation ensembles [33], apply univariate classifiers to each channel separately and combine their predictions. In contrast, cross-channel methods aim to capture the dependencies and interactions between different channels. For example, the multivariate extensions of ROCKET [34] have demonstrated strong performance by explicitly considering cross-channel information during the transformation process.

3 Methodology

This work enhances the DLN framework, originally proposed for tabular classification [3] and later adapted to regression [4], and applies it to the TSC domain. The complete workflow, called TSC-DLN and shown in Fig. 2, begins with data transformation, followed by a hyperparameter search, and concludes with model training and evaluation. Compared to our earlier DLN variants, two modifications are required:

1. Feature extraction for time series: Raw, variable-length sequences are converted to fixed-length tabular vectors.
2. Automated architectural search: Several design choices (two-phase vs. unified training, search-space pruning, use of straight-through estimators, and input concatenation) are no longer hard-coded but are selected automatically through hyperparameter optimization.

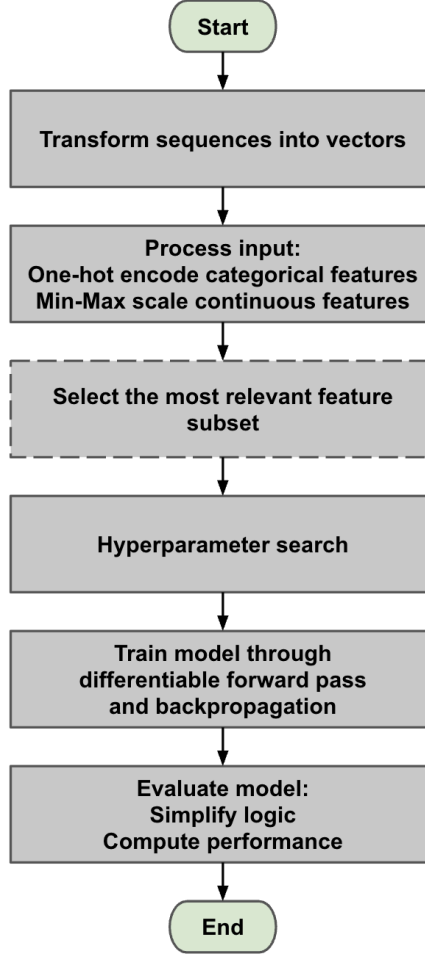


Figure 2: Experimental workflow for TSC-DLN.

3.1 Time-series Feature-based Transformation

To apply our tabular DLN model, we first transform each variable-length time series into a fixed-dimension feature vector. We explore the following two feature extraction methods:

- **Catch22** [5]: This method transforms any time series into a canonical and efficient set of 22 features, capturing a wide range of sequence properties.
- **TSFresh** [6]: This method generates a comprehensive set of features. To ensure relevance and reduce dimensionality, we then employ cross-validated random forests to select the most salient features, creating feature vectors of size 10, 20, or 40.

The resulting feature vector is then scaled to have values within $[0, 1]$ and serves as the DLN input.

Table 1: Trainable parameters and forward equations of the proposed TSC-DLN. Blue entries (●) are *neuron-function* weights; red entries (●) are *connection* weights. \mathbf{x} / \mathbf{y} denote layer input / output, τ is the shared temperature during training, and $\theta_{\text{sum}}=0.8$.

	Trainable parameters	Training forward (differentiable)	Inference forward (discrete)
Threshold Layer	<ul style="list-style-type: none"> ● bias $\mathbf{b} \in \mathbb{R}^{\text{in}}$ ● slope $\mathbf{s} \in \mathbb{R}^{\text{in}}$ 	$\mathbf{y}_i = \text{Sigmoid}(\mathbf{s}_i (\mathbf{x}_i - \mathbf{b}_i) / \tau)$	$\mathbf{y}_i = \text{Heaviside}(\mathbf{s}_i (\mathbf{x}_i - \mathbf{b}_i))$
Logic Layer	<ul style="list-style-type: none"> ● logic-fn weights $\mathbf{W} \in \mathbb{R}^{\text{out} \times 16}$ ● link-a weights $\mathbf{U} \in \mathbb{R}^{\text{out} \times \text{in}}$ ● link-b weights $\mathbf{V} \in \mathbb{R}^{\text{out} \times \text{in}}$ 	$P = \text{Softmax}(\mathbf{W}_{i,:} / \tau)$ $a = \sum_j [\text{Softmax}(\mathbf{U}_{i,:} / \tau)]_j \mathbf{x}_j$ $b = \sum_j [\text{Softmax}(\mathbf{V}_{i,:} / \tau)]_j \mathbf{x}_j$ $\mathbf{y}_i = \sum_{k=0}^{15} P_k \text{SoftLogic}_k(a, b)$	$k = \arg \max_j \mathbf{W}_{i,j}$ $a_i = \arg \max_j \mathbf{U}_{i,j}$ $b_i = \arg \max_j \mathbf{V}_{i,j}$ $\mathbf{y}_i = \text{HardLogic}_k(\mathbf{x}_{a_i}, \mathbf{x}_{b_i})$
Sum Layer	<ul style="list-style-type: none"> ● link weights $\mathbf{S} \in \mathbb{R}^{\text{in} \times C}$ 	$\mathbf{y}_c = \sum_j \text{Sigmoid}(\mathbf{S}_{j,c} / \tau) \mathbf{x}_j$	$\mathbf{y}_c = \sum_j 1_{\{\text{Sigmoid}(\mathbf{S}_{j,c} / \tau) \geq \theta_{\text{sum}}\}} \mathbf{x}_j$

3.2 Differentiable Logic Network

The DLN follows the three-layer template, as illustrated in Fig. 1:

1. **ThresholdLayer**: Differentiable binarization of continuous inputs. Each input is linked to a predefined number of threshold neurons (10 or 14 in our experiments), with the layer learning the optimal cutoff value for each one.
2. **LogicLayer(s)**: Sparse, two-input Boolean neurons that enable nonlinearity and interpretability. For each neuron, the layer learns its logic operation and which two outputs from the previous layer serve as its inputs.
3. **SumLayer**: Class-wise aggregation of the final LogicLayer’s activations. This layer learns which of these activations (i.e., logic rules) to sum up for each class to produce the final scores.

To enable gradient-based training, we employ the same differentiable relaxation techniques as in our prior work. Discrete choices, such as selecting a logic function for a neuron or its input connections, are relaxed into continuous, probabilistic mixtures using softmax or sigmoid functions. Table 1 summarizes the layer-wise parameters and their forward-pass computations. Trainable parameters are color-coded: blue for neuron function weights and red for connection weights. We now detail the forward equations of each DLN layer, both during training (differentiable relaxations) and during inference (discrete execution).

Notation. Let $\mathbf{x} \in [0, 1]^{\text{in}}$ be a layer input and \mathbf{y} its output, τ the common decaying temperature during training, and $\theta_{\text{sum}}=0.8$ the fixed connectivity threshold used by the SumLayer at inference.

ThresholdLayer. During training, each neuron applies a temperature-scaled sigmoid,

$$\mathbf{y}_i = \text{Sigmoid}(\mathbf{s}_i (\mathbf{x}_i - \mathbf{b}_i) / \tau),$$

where \mathbf{b}_i and \mathbf{s}_i are its learnable bias and slope, respectively. At inference time, the layer is discretised to a hard threshold,

$$\mathbf{y}_i = \text{Heaviside}(\mathbf{s}_i (\mathbf{x}_i - \mathbf{b}_i)).$$

Each continuous input is connected to a group of threshold neurons. The biases for these neurons are initialized using the bin edges from a decision tree trained on that input feature and their slopes are initialized to a value of 2. After training, any neurons with bias values pushed beyond the input

Table 2: List of all real-valued binary logic operations. Adapted from LGN [1].

ID	Operator	Real-valued	00	01	10	11
0	False	0	0	0	0	0
1	$A \wedge B$	$A \cdot B$	0	0	0	1
2	$\neg(A \Rightarrow B)$	$A - AB$	0	0	1	0
3	A	A	0	0	1	1
4	$\neg(A \Leftarrow B)$	$B - AB$	0	1	0	0
5	B	B	0	1	0	1
6	$A \oplus B$	$A + B - 2AB$	0	1	1	0
7	$A \vee B$	$A + B - AB$	0	1	1	1
8	$\neg(A \vee B)$	$1 - (A + B - AB)$	1	0	0	0
9	$\neg(A \oplus B)$	$1 - (A + B - 2AB)$	1	0	0	1
10	$\neg B$	$1 - B$	1	0	1	0
11	$A \Leftarrow B$	$1 - B + AB$	1	0	1	1
12	$\neg A$	$1 - A$	1	1	0	0
13	$A \Rightarrow B$	$1 - A + AB$	1	1	0	1
14	$\neg(A \wedge B)$	$1 - AB$	1	1	1	0
15	True	1	1	1	1	1

range of $[0, 1]$ are treated as constant **True** or **False** values. Experimental results show that this design enables the DLN to perform efficient feature selection.

LogicLayer. Each LogicLayer neuron realizes one of the 16 possible two-input Boolean functions. A complete lookup table, adapted from the LGN paper, is provided in Table 2. Training employs the differentiable real-valued logic SoftLogic_k, while inference switches to the binary logic of HardLogic_k. For example,

$$\text{SoftLogic}_{\text{AND}}(a, b) = ab,$$

$$\text{HardLogic}_{\text{AND}}(a, b) = 1_{\{a=1\}} 1_{\{b=1\}}.$$

Let

$$P_k = \text{Softmax}(\mathbf{W}_{i,:}/\tau)_k,$$

$$\alpha_j = \text{Softmax}(\mathbf{U}_{i,:}/\tau)_j,$$

$$\beta_j = \text{Softmax}(\mathbf{V}_{i,:}/\tau)_j,$$

select, respectively, the Boolean operator and the two incoming signals. Training employs the differentiable relaxation

$$a = \sum_j \alpha_j \mathbf{x}_j,$$

$$b = \sum_j \beta_j \mathbf{x}_j,$$

$$\mathbf{y}_i = \sum_{k=0}^{15} P_k \text{SoftLogic}_k(a, b).$$

Inference quantizes all three categorical choices,

$$k^* = \arg \max_k \mathbf{W}_{i,k},$$

$$a^* = \arg \max_j \mathbf{U}_{i,j},$$

$$b^* = \arg \max_j \mathbf{V}_{i,j},$$

and evaluates the corresponding hard gate,

$$\mathbf{y}_i = \text{HardLogic}_{k^*}(\mathbf{x}_{a^*}, \mathbf{x}_{b^*}).$$

SumLayer. For each class $c \in \{1, \dots, C\}$, the output logit during training is

$$\mathbf{y}_c = \sum_j \text{Sigmoid}(\mathbf{S}_{j,c}/\tau) \mathbf{x}_j,$$

where \mathbf{S} contains the (logit) connection strengths. At inference time, the connectivity pattern is binarized using $\theta_{\text{sum}} = 0.8$:

$$\mathbf{y}_c = \sum_j \mathbf{1}_{\{\text{Sigmoid}(\mathbf{S}_{j,c}/\tau) \geq \theta_{\text{sum}}\}} \mathbf{x}_j.$$

The final class prediction is:

$$\hat{y} = \arg \max_c \mathbf{y}_c.$$

After the model is trained, we extract the learned logic rules and simplify them using SymPy [35] to reduce model complexity and enhance interpretability.

3.3 Hyperparameter-driven Methodological Choices

A primary contribution of this work is to delegate several key methodological decisions to the HPO process. While previous work fixes these settings and evaluates them in ablation studies, we incorporate them into a unified search space. This empowers the HPO algorithm to discover the optimal configuration for each dataset with a 128-trial search. The choices automated by HPO include:

- **Training Strategy:** Optimization can proceed either via the two-phase approach from our original work (learning neuron functions and connections alternately) or the unified end-to-end approach from our regression DLN (learning both simultaneously). This is controlled by a Boolean flag.
- **Search Subspacing:** To manage complexity and improve gradient flow, we can constrain the search for logic functions and input connections. The HPO process selects the subspace size for logic gate functions from $\{16, 8, 4\}$ candidates and for neuron links from $\{16, 8, 4, 2, 1\}$ candidates.
- **Straight-through Estimators (STEs):** To mitigate the impact of vanishing gradients and concentrated activations from cascaded relaxation functions while maintaining a discrete forward pass, we treat the use of STEs [36] for each of the three layer types (Threshold, Logic, and Sum) as a Boolean hyperparameter.
- **Input Concatenation:** Inspired by the Wide & Deep model [37], we test the efficacy of creating shortcut connections by concatenating the ThresholdLayer’s output to the input of each subsequent LogicLayer. This is also controlled by a Boolean HPO flag.

4 Experiments

We evaluate our TSC-DLN framework against eight baseline methods on 51 TSC datasets from the UCR Time-Series Classification Archive [8]. The baselines are k -nearest neighbors (KNN), Gaussian Naive Bayes (NB), logistic regression (LR), support vector machine (SVM), decision tree (DT), AdaBoost (AB), random forest (RF), and a multilayer perceptron (MLP). In Appendix A, Table 5

provides the characteristics (training set size, test set size, number of classes, and number of continuous and categorical features for Catch22 and TSFresh variants) of each dataset after transformation and processing. Sample sizes range from hundreds to thousands and input dimensions range from 10 to 40. We evaluate models based on balanced accuracy and inference cost and illustrate the DLN’s interpretability by providing examples of its decision-making processes. As summarized in Fig. 3, the DLN lies on the Pareto frontier under every transformation setting. Inference OPs refers to the number of logic-gate operations in the model (details given later).

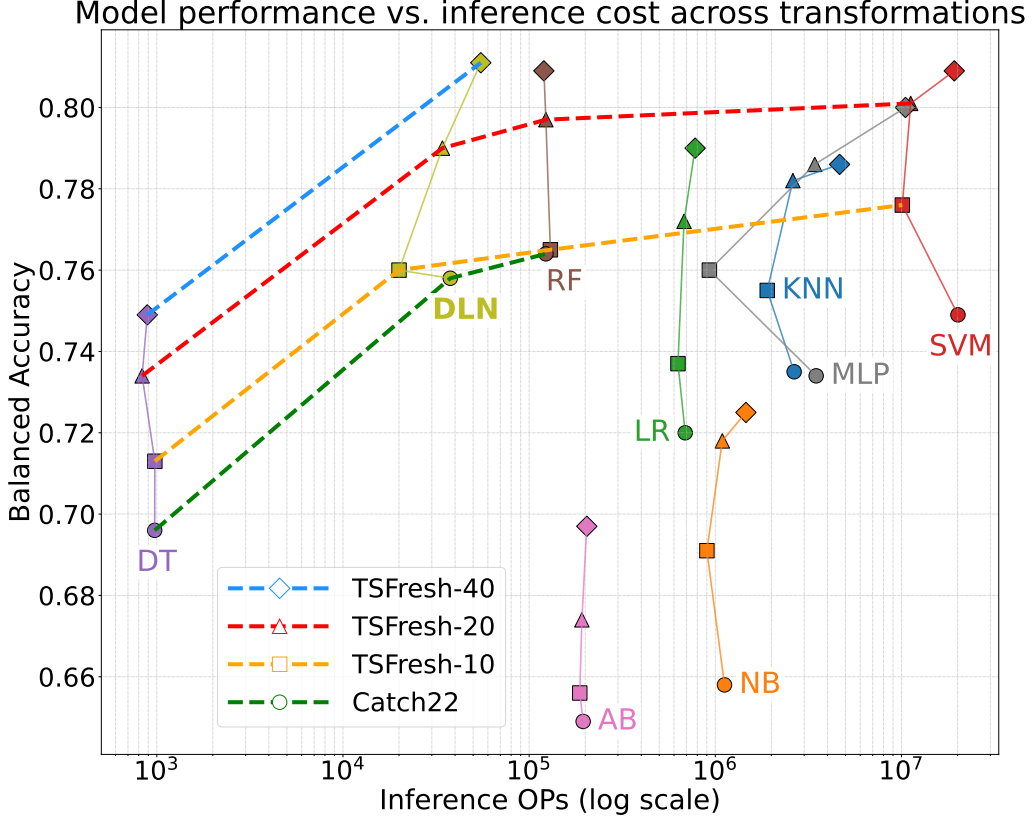


Figure 3: Average balanced accuracy (best of 10 runs) versus inference operation cost for all models across 51 datasets. Results are shown for the Catch22, TSFresh-10, TSFresh-20, and TSFresh-40 transformations, with the Pareto frontier drawn for each case. The DLN is Pareto-optimal in every instance and is the top-performing model with the TSFresh-40 transformation.

4.1 Experimental Setup

We select 51 datasets from the 128 available in the UCR Archive based on the following criteria:

- The dataset has no empty dimensions.
- No missing values are present.
- All sequences in both the training and test sets have the same length.
- The training set contains between 100 and 10,000 samples.
- The test set contains at least 100 samples.

- Every class has at least 5 samples in both the training and test sets.

Because the UCR Archive already provides train-test splits, we use those splits directly.

Each dataset is then preprocessed as follows:

1. Convert every time-series sequence into a feature vector with the chosen transformation method.
2. Remove columns that contain NaNs (not a number) after transformation, as some features may not be applicable to every dataset.
3. Remove duplicate rows and constant features.
4. When feature selection is required (e.g., for TSFresh), rank features in the training set with cross-validated random forests and keep the most informative subset.
5. One-hot encode categorical variables; we treat both originally categorical variables and continuous variables with too few unique values as categorical.
6. Clip outliers and apply min-max scaling to continuous features so they fall within the $[0, 1]$ range.

Detailed dataset characteristics after selection, transformation, and preprocessing are provided in Table 5.

For every dataset-transformation-model combination, we run 10 independent experiments, each with a distinct random seed. Each run begins with a hyperparameter search in which Optuna [38] samples configurations from a predefined grid; the configuration that yields the highest cross-validated balanced accuracy is retained. Each model type shares the same HPO search space for every dataset-transformation pair. We employ two to four cross-validation folds, allocating more folds to smaller datasets. The search space includes parameters for both model structure (e.g., DLN’s hidden sizes and DT’s maximum height) and learning optimizations (e.g., DLN’s learning rate and SVM’s kernel type). After selecting the optimal hyperparameters, we train the model and then evaluate it on the held-out test split. We use scikit-learn [39] for traditional models and PyTorch [40] for neural network models. In addition, aeon [41] handles dataset loading and basic time-series processing, scikit-learn manages tabular preprocessing, and Ray [42, 43] orchestrates parallel HPO and training jobs.

4.2 Accuracy

For each dataset-transformation-model combination, we record the test balanced accuracies of 10 independent runs. We are interested in both the numerical values and the *ease* of finding a well-performing model, which is reflected, for example, in the best accuracy achieved across 10 runs. We report the best-out-of-10 and mean accuracies and corresponding ranks in Tables 3 and 4. For each transformation type, we present the average across all datasets.

Overall, the DLN performs well. In inference OPs, only DT outranks it. In best-out-of-10 balanced test accuracy, it ranks first, second or third. It improves considerably with more trials. It is particularly competitive among non-ensemble methods, outperforming the MLP in three cases and tying it once. Among the transformations, TSFresh yields better results than Catch22 on an average, and model performance generally improves as more features are used. Traditional methods like RF and SVM achieve strong accuracy. The DLN paired with the TSFresh-40 transformation emerges as the highest-performing combination when evaluated over multiple runs. Detailed results for each dataset-model pair for the Catch22, TSFresh-10, TSFresh-20, and TSFresh-40 transformations are reported in Appendices B, C, D, and E, respectively.

We also plot the *Best@k* curves for the five strongest models, defined as the expected maximum accuracy from k draws (without replacement) out of the 10 runs. The closed-form expression is

$$\mathbb{E}[\text{Best@k}] = \sum_{i=k}^n \frac{\binom{i-1}{k-1}}{\binom{n}{k}} x_{(i)},$$

where $n = 10$ is the total number of runs and $x_{(i)}$ denotes the i -th order statistic (accuracies sorted in ascending order). The *Best@k* is the mean when $k = 1$ and the best-out-of-10 when $k = 10$. We present the *Best@k* curves after the TSFresh-40 transformation in Fig. 4 and provide the curves for the remaining transformations in the Appendix. DLN exhibits the fastest-growing curve, indicating that running more trials is generally beneficial for finding a high-performing DLN. It also achieves the best overall performance when $k \geq 7$, demonstrating the potential of the DLN when given a sufficient number of trials.

Table 3: **Best-out-of-10** test balanced accuracy and corresponding inference operations (OPs), with rank (R: lower is better) computed for both. All values are averaged across datasets: accuracy and rank use an arithmetic mean, while OPs use a geometric mean. OPs are calculated assuming FP16 for floating-point and INT16 for integer arithmetic.

Transform.	Metric	Model								
		KNN	NB	LR	SVM	DT	RF	AB	MLP	DLN
Catch22	Acc \uparrow	0.735	0.658	0.720	0.749	0.696	0.764	0.649	0.734	0.758
	Acc R \downarrow	4.75	7.83	5.52	3.54	6.76	2.50	6.94	4.65	2.50
	Cost \downarrow	2.65M	1.12M	689K	20.1M	974	123K	195K	3.48M	37.7K
	Cost R \downarrow	6.92	6.41	4.96	8.76	1.00	3.22	3.90	7.69	2.14
TSFresh-10	Acc \uparrow	0.755	0.691	0.737	0.776	0.713	0.765	0.656	0.760	0.760
	Acc R \downarrow	4.55	7.23	5.12	2.51	6.93	3.41	7.09	4.14	4.03
	Cost \downarrow	1.90M	901K	630K	10.1M	976	130K	187K	929K	20.0K
	Cost R \downarrow	7.25	6.96	5.41	8.47	1.00	3.37	4.02	6.51	2.00
TSFresh-20	Acc \uparrow	0.782	0.718	0.772	0.801	0.734	0.797	0.674	0.786	0.790
	Acc R \downarrow	4.56	7.35	4.99	2.88	6.96	3.33	7.10	4.32	3.50
	Cost \downarrow	2.61M	1.09M	679K	11.2M	834	123K	192K	3.42M	34.2K
	Cost R \downarrow	7.14	6.39	5.04	8.51	1.00	3.24	3.86	7.75	2.08
TSFresh-40	Acc \uparrow	0.786	0.725	0.790	0.809	0.749	0.809	0.697	0.800	0.811
	Acc R \downarrow	5.10	7.66	5.14	3.05	6.92	3.62	6.66	3.96	2.90
	Cost \downarrow	4.65M	1.46M	779K	19.2M	889	120K	204K	10.5M	55.0K
	Cost R \downarrow	7.14	6.20	4.86	8.47	1.00	3.12	3.90	8.12	2.20

Table 4: **Mean** test balanced accuracy and inference operations (OPs) averaged over 10 random seeds, with ranks computed for both metrics. Accuracy and rank are arithmetically averaged across datasets, while OPs are geometrically averaged. The OP calculation assumes FP16 for floating-point and INT16 for integer arithmetic.

Transform.	Metric	Model								
		KNN	NB	LR	SVM	DT	RF	AB	MLP	DLN
Catch22	Acc \uparrow	0.721	0.657	0.705	0.731	0.672	0.743	0.616	0.707	0.731
	Acc R \downarrow	4.31	7.22	5.03	3.10	6.99	2.78	6.91	5.54	3.12
	Cost \downarrow	2.88M	1.12M	689K	20.9M	1.00K	121K	212K	4.37M	38.6K
	Cost R \downarrow	6.92	6.31	4.88	8.82	1.00	3.00	4.24	7.76	2.06
TSFresh-10	Acc \uparrow	0.743	0.691	0.726	0.759	0.690	0.745	0.626	0.732	0.735
	Acc R \downarrow	3.97	6.21	4.65	2.41	7.09	3.66	7.29	4.98	4.75
	Cost \downarrow	2.53M	901K	630K	16.4M	942	113K	205K	1.19M	18.6K
	Cost R \downarrow	7.33	6.65	5.18	8.86	1.00	3.08	4.18	6.73	2.00
TSFresh-20	Acc \uparrow	0.768	0.718	0.759	0.786	0.711	0.777	0.647	0.762	0.767
	Acc R \downarrow	4.14	6.54	4.64	2.72	7.24	3.56	7.02	4.92	4.24
	Cost \downarrow	3.36M	1.09M	679K	18.3M	901	115K	210K	3.90M	35.5K
	Cost R \downarrow	7.08	6.27	4.96	8.78	1.00	2.98	4.18	7.69	2.06
TSFresh-40	Acc \uparrow	0.775	0.725	0.773	0.795	0.723	0.792	0.666	0.779	0.787
	Acc R \downarrow	4.74	6.84	4.86	2.77	7.26	3.61	6.84	4.31	3.75
	Cost \downarrow	5.73M	1.46M	779K	24.3M	901	117K	208K	13.4M	63.7K
	Cost R \downarrow	7.18	6.10	4.94	8.63	1.00	2.94	4.06	8.04	2.12

4.3 Efficiency

We assess inference efficiency by quantifying the total number of basic hardware logic-gate operations (OPs) required for a single prediction, following the methodology established in the original DLN article [3]. It involves translating a model’s high-level computational steps (e.g., floating-point arithmetic, comparisons) into their fundamental logic gate equivalents. For this conversion, we define the cost of each gate type: a two-input AND, OR, NAND, or NOR gate counts as one OP, whereas a two-input XOR or XNOR gate counts as three OPs. NOT gates are considered to have zero cost. To ensure a fair comparison across all models, our analysis assumes a standardized precision of 16 bits for both floating-point and integer data types. While models are trained using larger default precisions (e.g., float32 or float64), they typically maintain performance when downscaled. This assumption creates a consistent baseline but also conservatively estimates the advantage of logic-heavy models like the DLN, whose efficiency benefits are more pronounced when using larger, more costly data types.

The operational costs are also summarized in Tables 3 and 4. DLNs are highly efficient, second only to single decision trees in all cases, and lie on the Pareto frontier in the accuracy-versus-inference-cost plot shown in Fig. 3. On an average, they are several times more computationally efficient than strong-performing models like random forests and orders of magnitude more efficient than SVMs. The

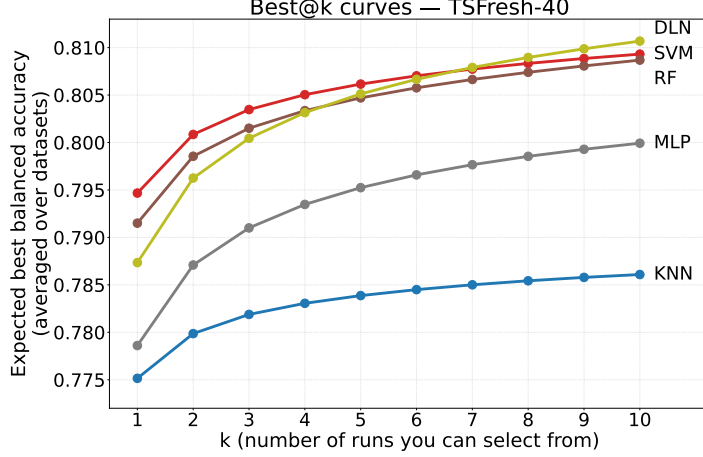


Figure 4: *Best@k* curves for the five strongest models using the TSFresh-40 transformation. The DLN curve exhibits the fastest growth and achieves the best overall performance, given a sufficient number of trials ($k \geq 7$).

sizes of NN-based models (i.e., DLN and MLP) are more impacted by the input size because their HPO search spaces are defined based on the input dimension.

4.4 Hyperparameter Analysis

Unlike previous tabular DLN studies, which fix many model-training configurations before HPO and ablate them afterward, we include these configurations directly in the HPO search space. They are:

- **phase_unified**: whether to learn functionality and connections simultaneously or alternately; a value of 1 denotes simultaneous learning.
- **ste_threshold_layer**: whether to apply STE when training the *ThresholdLayer*.
- **ste_logic_layer**: whether to apply STE when training the *LogicLayer*.
- **ste_sum_layer**: whether to apply STE when training the *SumLayer*.
- **subset_gate_num**: the number of candidate logic gates considered when learning a logic neuron’s functionality. Options are 16, 8, and 4, where 16 is the full set.
- **subset_link_num**: the number of candidate input links evaluated for each of the two links (a and b) in every logic neuron. Options are 16, 8, 4, 2, and 1; a value of 1 initializes a link once and then keeps it fixed.
- **concat_input**: whether to concatenate an input-*ThresholdLayer* pair to each hidden *LogicLayer*.

We summarize the statistics and show the HPO algorithm’s final choices in Fig. 5. For each transformation type, 510 experiments are carried out in all. Our findings are consistent with those for tabular classification DLNs: (i) alternating training is slightly better than updating both parameter types jointly; (ii) applying STE to all three layer types is beneficial; and (iii) concatenating the *ThresholdLayer*’s output is important. Furthermore, for the logic neurons, gate subsetting is usually selected, and it is preferable *not* to use an initialize-then-fix strategy for the links. Based on the combination statistics, a configuration with 8 candidate gates and 16 candidate links is the most common, although no single setting is significantly more frequent than the others.

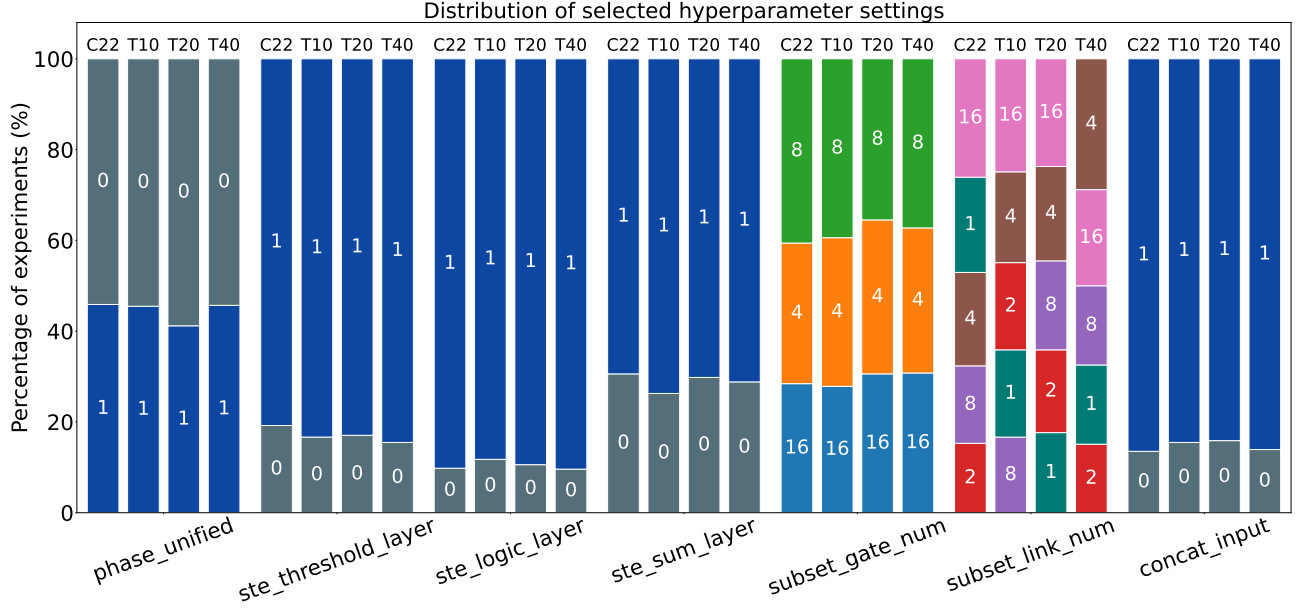


Figure 5: Distribution of model training configurations selected by the HPO algorithm for each of the four transformation methods. The statistics are aggregated across all (dataset, random seed) pairs, with each bar representing results from $51 \times 10 = 510$ experiments.

4.5 Interpretability

A key strength of the DLN architecture is its inherent interpretability. Once trained, a DLN can be visualized directly as a transparent, rule-based system. We illustrate this with models learned on the *FreezerRegularTrain* dataset using Catch22 and TSFresh-20 features in Figs. 6a and 6b, respectively. In these diagrams, the decision-making path is explicit. The process begins with input features (yellow rectangles), which are binarized against learned thresholds. These binary signals then propagate through a network of logic operators (diamonds) that formulate logic rules. The final output is an aggregation of the outputs from these rules. These networks are not only interpretable but also achieve strong performance while using only a small fraction of the available features, mirroring the feature selection behavior observed for tabular DLNs [3, 4].

4.6 Limitations

Although fast at inference, DLN training is slow. This is because the summation of real-valued logic operations in each logic neuron is not specifically accelerated by CUDA; this calculation also relies on the output of three preceding softmax functions. This makes applying DLNs to high-dimensional problems challenging. In our experiments, due to computational limitations, we used only up to 40 continuous features selected from the TSFresh transformation, which has benchmarks with more than 700 features. Furthermore, in the HPO stage, DLN has a large search space due to its many training configurations. HPO is more efficient on a refined search space when the number of trials is limited. Thus, whether a universally optimal configuration exists that can reduce the search space remains an open question.

Table 5: Dataset characteristics after transformation and preprocessing.

dataset	# train	# test	# class	Catch22		TSFresh-10		TSFresh-20		TSFresh-40	
				con.	cat.	con.	cat.	con.	cat.	con.	cat.
ACSF1	100	100	10	15	14	10	0	20	0	40	0
ChlorineConcentration	467	3840	3	22	0	10	0	20	0	40	0
Computers	250	250	2	21	0	10	0	20	0	40	0
CricketX	390	390	12	22	0	10	0	20	0	40	0
CricketY	390	390	12	22	0	10	0	20	0	40	0
CricketZ	390	390	12	22	0	10	0	20	0	40	0
Earthquakes	322	139	2	22	0	6	4	14	4	34	4
EOGHorizontalSignal	362	362	12	22	0	10	0	20	0	40	0
EOGVerticalSignal	362	362	12	22	0	10	0	20	0	40	0
EthanolLevel	504	500	4	19	0	10	0	20	0	40	0
FaceAll	560	1688	14	22	0	10	0	20	0	40	0
Fish	175	175	7	19	0	10	0	20	0	39	3
FordA	3601	1320	2	22	0	10	0	20	0	40	0
FordB	3636	810	2	22	0	9	0	19	0	39	0
FreezerRegularTrain	150	2846	2	20	5	10	0	20	0	40	0
GunPointAgeSpan	135	316	2	21	3	10	0	19	2	39	2
GunPointMaleVersusFemale	135	316	2	21	3	9	2	19	2	39	2
GunPointOldVersusYoung	136	315	2	21	2	8	4	18	4	38	4
Ham	109	105	2	22	0	10	0	20	0	40	0
HandOutlines	1000	370	2	19	0	10	0	20	0	39	0
Haptics	155	308	5	22	0	10	0	20	0	40	0
InlineSkate	99	521	7	20	3	10	0	20	0	40	0
InsectWingbeatSound	220	1980	11	22	0	10	0	20	0	40	0
LargeKitchenAppliances	375	375	3	22	0	10	0	20	0	40	0
MixedShapesRegularTrain	500	2420	5	21	0	10	0	20	0	40	0
MixedShapesSmallTrain	100	2420	5	21	0	10	0	20	0	40	0
NonInvasiveFetalECGThorax1	1800	1965	42	22	0	10	0	20	0	40	0
NonInvasiveFetalECGThorax2	1800	1965	42	22	0	10	0	20	0	40	0
OSULeaf	200	242	6	22	0	10	0	20	0	40	0
Plane	105	105	7	22	0	10	0	20	0	40	0
PowerCons	145	145	2	22	0	9	2	19	2	39	2
RefrigerationDevices	375	375	3	22	0	10	0	20	0	39	2
ScreenType	375	375	3	21	0	10	0	20	0	40	0
SemgHandGenderCh2	300	600	2	22	0	10	0	20	0	40	0
SemgHandMovementCh2	450	450	6	22	0	10	0	20	0	40	0
SemgHandSubjectCh2	450	450	5	22	0	10	0	20	0	40	0
ShapesAll	600	600	60	22	0	10	0	19	2	39	2
SmallKitchenAppliances	375	375	3	22	0	10	0	20	0	40	0
StarLightCurves	1000	8236	3	21	0	10	0	20	0	40	0
Strawberry	613	370	2	19	6	10	0	20	0	40	0
SwedishLeaf	500	624	15	22	0	10	0	20	0	40	0
Trace	100	100	4	20	3	7	2	15	2	34	4
TwoPatterns	1000	4000	4	22	0	10	0	20	0	40	0
UWaveGestureLibraryAll	896	3582	8	22	0	10	0	20	0	40	0
UWaveGestureLibraryX	896	3582	8	22	0	10	0	20	0	40	0
UWaveGestureLibraryY	896	3582	8	22	0	10	0	20	0	40	0
UWaveGestureLibraryZ	896	3582	8	18	0	10	0	20	0	40	0
Wafer	1000	6164	2	22	0	10	0	20	0	40	0
Worms	158	77	5	22	0	10	0	20	0	40	0
WormsTwoClass	158	77	2	22	0	9	0	19	0	39	0
Yoga	300	3000	2	21	3	9	2	19	2	39	2

B Detailed Results for Catch22

In this section, we present the accuracy and inference-cost results for each dataset obtained with Catch22. Fig. 7 depicts the *Best@k* curves for the five strongest models, acting as the Catch22 counterpart to Fig. 4. Table 6 reports the best-of-10 test balanced accuracy and serves as a detailed reference for Table 3. Table 7 provides the dataset-wise mean test balanced accuracy averaged over 10 runs, corresponding to Table 4. Table 8 lists the geometric mean number of OPs required during inference. A concise summary of these figures appears in Table 4.

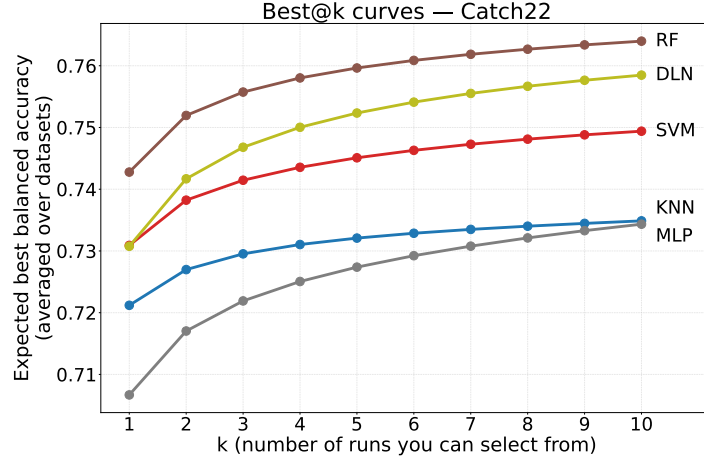


Figure 7: The *Best@k* curves for the five strongest models on Catch22. DLN’s curve grows the fastest.

C Detailed Results for TSFresh-10

This section reports the accuracy and inference-cost metrics obtained with the TSFresh-10 feature transformation. Fig. 8 illustrates the *Best@k* curves for the five strongest models, serving as the TSFresh-10 counterpart to Fig. 4. Table 9 lists the best-of-10 test balanced accuracies and serves as a detailed counterpart to Table 3. Table 10 shows the mean test balanced accuracy across 10 runs for every dataset, corresponding to Table 4. Finally, Table 11 provides the geometric mean number of OPs required during inference; a concise summary of these values is included in Table 4.

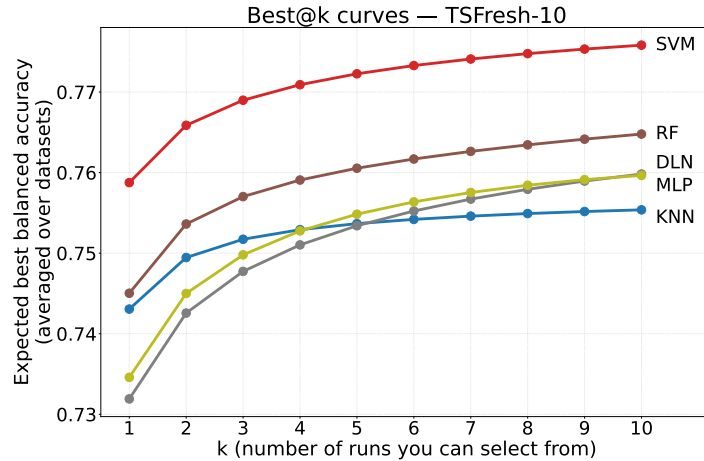


Figure 8: The *Best@k* curves for the five strongest models on TSFresh-10.

D Detailed Results for TSFresh-20

Analogous results for the TSFresh-20 feature transformation are presented next. Fig. 9 shows the *Best@k* curves for the five strongest models, constituting the TSFresh-20 counterpart to Fig. 4. Table 12 lists the best-of-10 test balanced accuracies, complementing Table 3. Dataset-wise mean test balanced accuracies averaged over 10 runs appear in Table 13, providing the detailed values summarized in Table 4. Table 14 presents the geometric mean OP count during inference; its condensed summary is found in Table 4.

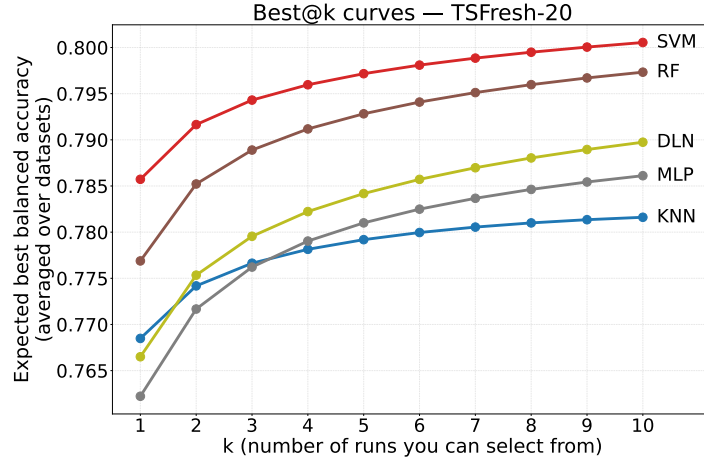


Figure 9: The *Best@k* curves for the five strongest models on TSFresh-20.

E Detailed Results for TSFresh-40

Finally, we report the metrics for the TSFresh-40 feature transformation. Table 15 details the best-of-10 test balanced accuracies, corresponding to Table 3. Table 16 lists the mean test balanced accuracies across 10 runs for each dataset, providing the dataset-level figures summarized in Table 4. Table 17 reports the geometric mean number of OPs required at inference time; a summary of these results is included in Table 4.

Table 6: Best-of-10 test balanced accuracy for Catch22.

	KNN	NB	LR	SVM	DT	RF	AB	MLP	DLN
ACSF1	0.790	0.710	0.740	0.760	0.690	0.850	0.580	0.750	0.770
ChlorineConcentration	0.499	0.394	0.388	0.496	0.423	0.457	0.402	0.477	0.465
Computers	0.712	0.684	0.720	0.752	0.708	0.732	0.740	0.728	0.736
CricketX	0.597	0.451	0.501	0.579	0.457	0.573	0.413	0.527	0.574
CricketY	0.550	0.411	0.481	0.551	0.383	0.533	0.397	0.498	0.538
CricketZ	0.599	0.443	0.520	0.573	0.432	0.616	0.371	0.541	0.566
Earthquakes	0.580	0.684	0.693	0.674	0.641	0.703	0.552	0.609	0.689
EOGHorizontalSignal	0.495	0.445	0.521	0.491	0.417	0.580	0.376	0.501	0.525
EOGVerticalSignal	0.454	0.373	0.421	0.432	0.403	0.499	0.353	0.414	0.456
EthanolLevel	0.328	0.312	0.374	0.388	0.339	0.352	0.368	0.400	0.396
FaceAll	0.643	0.570	0.689	0.684	0.569	0.741	0.501	0.668	0.730
Fish	0.769	0.614	0.793	0.775	0.640	0.769	0.623	0.777	0.796
FordA	0.875	0.699	0.860	0.901	0.909	0.917	0.913	0.913	0.917
FordB	0.738	0.586	0.665	0.751	0.731	0.730	0.745	0.762	0.774
FreezerRegularTrain	0.961	0.867	0.996	0.996	0.997	0.998	0.997	0.995	0.998
GunPointAgeSpan	0.936	0.805	0.915	0.953	0.946	0.978	0.965	0.940	0.959
GunPointMaleVersusFemale	1.00	0.984	0.997	0.997	0.978	0.991	0.978	0.997	1.00
GunPointOldVersusYoung	1.00	0.988	1.00	1.00	1.00	1.00	1.00	1.00	1.00
Ham	0.678	0.511	0.725	0.743	0.628	0.641	0.629	0.704	0.697
HandOutlines	0.797	0.622	0.816	0.845	0.809	0.851	0.813	0.847	0.836
Haptics	0.424	0.374	0.430	0.430	0.397	0.502	0.422	0.394	0.456
InlineSkate	0.420	0.341	0.376	0.388	0.369	0.473	0.322	0.392	0.382
InsectWingbeatSound	0.461	0.507	0.466	0.483	0.465	0.573	0.427	0.444	0.502
LargeKitchenAppliances	0.723	0.800	0.864	0.869	0.805	0.853	0.797	0.859	0.827
MixedShapesRegularTrain	0.901	0.839	0.884	0.895	0.858	0.912	0.868	0.886	0.906
MixedShapesSmallTrain	0.847	0.832	0.847	0.844	0.829	0.862	0.842	0.847	0.860
NonInvasiveFetalECGThorax1	0.765	0.766	0.816	0.849	0.712	0.822	0.208	0.801	0.820
NonInvasiveFetalECGThorax2	0.830	0.798	0.849	0.857	0.744	0.852	0.212	0.840	0.857
OSULeaf	0.661	0.618	0.700	0.734	0.575	0.684	0.581	0.712	0.762
Plane	0.991	0.912	0.938	0.959	0.944	1.00	0.949	0.954	0.991
PowerCons	0.917	0.897	0.924	0.931	0.883	0.931	0.952	0.931	0.945
RefrigerationDevices	0.539	0.525	0.533	0.587	0.536	0.536	0.504	0.597	0.536
ScreenType	0.456	0.389	0.477	0.493	0.507	0.523	0.531	0.488	0.515
SemgHandGenderCh2	0.915	0.742	0.822	0.899	0.876	0.903	0.872	0.904	0.917
SemgHandMovementCh2	0.718	0.427	0.556	0.682	0.649	0.778	0.578	0.698	0.760
SemgHandSubjectCh2	0.842	0.618	0.722	0.847	0.773	0.836	0.693	0.829	0.858
ShapesAll	0.718	0.688	0.632	0.677	0.575	0.727	0.123	0.600	0.717
SmallKitchenAppliances	0.755	0.741	0.811	0.795	0.763	0.819	0.797	0.803	0.816
StarLightCurves	0.931	0.885	0.937	0.943	0.946	0.947	0.943	0.939	0.946
Strawberry	0.913	0.705	0.865	0.929	0.891	0.926	0.880	0.918	0.917
SwedishLeaf	0.850	0.809	0.849	0.857	0.802	0.881	0.657	0.836	0.884
Trace	1.00	0.913	1.00	1.00	1.00	1.00	0.952	1.00	1.00
TwoPatterns	0.768	0.787	0.808	0.847	0.840	0.844	0.755	0.838	0.865
UWaveGestureLibraryAll	0.745	0.667	0.722	0.772	0.694	0.809	0.697	0.731	0.800
UWaveGestureLibraryX	0.712	0.664	0.692	0.732	0.674	0.747	0.628	0.698	0.736
UWaveGestureLibraryY	0.654	0.541	0.606	0.658	0.601	0.691	0.540	0.613	0.674
UWaveGestureLibraryZ	0.668	0.617	0.644	0.680	0.613	0.682	0.608	0.667	0.681
Wafer	0.962	0.969	0.979	0.980	0.983	0.995	0.992	0.981	0.992
Worms	0.765	0.635	0.675	0.703	0.574	0.705	0.536	0.669	0.709
WormsTwoClass	0.886	0.818	0.784	0.818	0.761	0.879	0.773	0.822	0.879
Yoga	0.740	0.582	0.678	0.739	0.737	0.762	0.716	0.712	0.753

Table 7: Mean and standard deviation of balanced accuracy for Catch22 across 10 random seeds.

	KNN	NB	LR	SVM	DT	RF	AB	MLP	DLN
ACSF1	0.758 ± 0.030	0.698 ± 0.018	0.687 ± 0.052	0.697 ± 0.028	0.655 ± 0.028	0.807 ± 0.033	0.441 ± 0.081	0.715 ± 0.028	0.728 ± 0.026
ChlorineConcentration	0.488 ± 0.010	0.394 ± 0.0	0.373 ± 8.5e-03	0.475 ± 0.031	0.411 ± 5.9e-03	0.435 ± 0.013	0.396 ± 5.0e-03	0.464 ± 0.011	0.440 ± 0.018
Computers	0.683 ± 0.024	0.684 ± 0.0	0.704 ± 0.015	0.723 ± 0.020	0.682 ± 0.029	0.711 ± 0.011	0.710 ± 0.017	0.682 ± 0.028	0.690 ± 0.024
CricketX	0.585 ± 0.011	0.451 ± 0.0	0.477 ± 0.017	0.561 ± 0.016	0.427 ± 0.034	0.550 ± 0.017	0.384 ± 0.017	0.507 ± 0.023	0.554 ± 0.017
CricketY	0.537 ± 7.2e-03	0.411 ± 0.0	0.472 ± 6.1e-03	0.534 ± 0.011	0.362 ± 0.013	0.515 ± 0.012	0.360 ± 0.019	0.476 ± 0.018	0.509 ± 0.026
CricketZ	0.591 ± 7.0e-03	0.443 ± 0.0	0.509 ± 6.4e-03	0.540 ± 0.016	0.417 ± 0.011	0.590 ± 0.015	0.344 ± 0.013	0.492 ± 0.031	0.530 ± 0.022
EOGHorizontalSignal	0.470 ± 0.013	0.444 ± 3.5e-03	0.488 ± 0.036	0.449 ± 0.029	0.383 ± 0.029	0.556 ± 0.013	0.287 ± 0.040	0.460 ± 0.034	0.489 ± 0.027
EOGVerticalSignal	0.414 ± 0.014	0.369 ± 5.4e-03	0.357 ± 0.027	0.394 ± 0.025	0.370 ± 0.017	0.480 ± 0.012	0.290 ± 0.040	0.376 ± 0.020	0.415 ± 0.027
Earthquakes	0.573 ± 0.012	0.684 ± 0.0	0.678 ± 0.021	0.638 ± 0.029	0.602 ± 0.022	0.674 ± 0.016	0.537 ± 0.010	0.559 ± 0.034	0.600 ± 0.052
EthanolLevel	0.313 ± 0.013	0.312 ± 0.0	0.366 ± 4.3e-03	0.370 ± 0.011	0.328 ± 0.012	0.338 ± 8.8e-03	0.350 ± 0.010	0.359 ± 0.019	0.371 ± 0.014
FaceAll	0.631 ± 9.4e-03	0.570 ± 0.0	0.684 ± 4.4e-03	0.667 ± 0.015	0.526 ± 0.025	0.716 ± 0.016	0.453 ± 0.033	0.642 ± 0.012	0.703 ± 0.023
Fish	0.721 ± 0.032	0.614 ± 0.0	0.750 ± 0.039	0.749 ± 0.015	0.600 ± 0.023	0.721 ± 0.037	0.604 ± 0.017	0.751 ± 0.026	0.748 ± 0.027
FordA	0.869 ± 2.9e-03	0.699 ± 0.0	0.857 ± 1.4e-03	0.897 ± 3.3e-03	0.905 ± 3.2e-03	0.905 ± 9.3e-03	0.908 ± 3.0e-03	0.894 ± 9.7e-03	0.909 ± 5.1e-03
FordB	0.714 ± 0.014	0.586 ± 0.0	0.661 ± 2.5e-03	0.745 ± 4.7e-03	0.714 ± 0.024	0.703 ± 0.029	0.733 ± 9.7e-03	0.729 ± 0.017	0.759 ± 9.3e-03
FreezerRegularTrain	0.957 ± 7.9e-03	0.866 ± 9.1e-04	0.996 ± 2.8e-04	0.996 ± 4.7e-04	0.997 ± 0.0	0.997 ± 3.4e-04	0.997 ± 0.0	0.987 ± 6.0e-03	0.988 ± 0.016
GunPointAgeSpan	0.934 ± 1.1e-03	0.800 ± 2.2e-03	0.892 ± 0.018	0.940 ± 0.019	0.922 ± 0.026	0.971 ± 4.8e-03	0.960 ± 3.6e-03	0.930 ± 9.5e-03	0.942 ± 0.018
GunPointMaleVersusFemale	0.999 ± 1.3e-03	0.981 ± 2.5e-03	0.995 ± 2.9e-03	0.994 ± 2.5e-03	0.976 ± 3.8e-03	0.984 ± 7.5e-03	0.975 ± 2.9e-03	0.992 ± 6.4e-03	0.995 ± 4.0e-03
GunPointOldVersusYoung	1.00 ± 9.6e-04	0.988 ± 0.0	1.00 ± 9.6e-04	1.00 ± 0.0	1.00 ± 0.0	1.00 ± 0.0	1.00 ± 0.0	0.999 ± 3.1e-03	1.00 ± 0.0
Ham	0.579 ± 0.044	0.511 ± 0.0	0.695 ± 0.017	0.689 ± 0.053	0.601 ± 0.021	0.615 ± 0.019	0.604 ± 0.020	0.662 ± 0.029	0.634 ± 0.047
HandOutlines	0.787 ± 0.015	0.622 ± 0.0	0.814 ± 5.0e-03	0.823 ± 0.013	0.786 ± 0.013	0.841 ± 7.3e-03	0.806 ± 6.0e-03	0.796 ± 0.020	0.820 ± 0.014
Haptics	0.410 ± 0.010	0.374 ± 0.0	0.399 ± 0.013	0.385 ± 0.031	0.356 ± 0.024	0.480 ± 0.017	0.406 ± 0.011	0.383 ± 0.013	0.430 ± 0.022
InlineSkate	0.411 ± 0.017	0.337 ± 4.0e-03	0.356 ± 0.023	0.379 ± 5.5e-03	0.339 ± 0.036	0.436 ± 0.022	0.293 ± 0.017	0.364 ± 0.024	0.353 ± 0.022
InsectWingbeatSound	0.444 ± 0.011	0.507 ± 0.0	0.450 ± 0.015	0.468 ± 0.011	0.436 ± 0.021	0.526 ± 0.032	0.405 ± 0.023	0.429 ± 0.011	0.488 ± 0.016
LargeKitchenAppliances	0.719 ± 7.9e-03	0.800 ± 0.0	0.849 ± 0.014	0.858 ± 5.8e-03	0.785 ± 0.011	0.840 ± 0.012	0.764 ± 0.023	0.826 ± 0.023	0.812 ± 0.011
MixedShapesRegularTrain	0.898 ± 4.2e-03	0.839 ± 0.0	0.879 ± 3.3e-03	0.890 ± 4.4e-03	0.849 ± 6.0e-03	0.901 ± 9.7e-03	0.864 ± 3.3e-03	0.875 ± 8.8e-03	0.897 ± 8.4e-03

continued on next page

Table 7 (continued)

	KNN	NB	LR	SVM	DT	RF	AB	MLP	DLN
MixedShapesSmallTrain	0.846 $\pm 5.2\text{e-}03$	0.832 ± 0.0	0.831 ± 0.019	0.830 $\pm 9.2\text{e-}03$	0.810 ± 0.013	0.851 $\pm 9.3\text{e-}03$	0.793 ± 0.072	0.830 $\pm 7.9\text{e-}03$	0.838 ± 0.015
NonInvasiveFetalECGThorax1	0.765 $\pm 1.8\text{e-}03$	0.765 $\pm 9.2\text{e-}04$	0.812 $\pm 3.7\text{e-}03$	0.842 $\pm 3.1\text{e-}03$	0.697 ± 0.012	0.797 ± 0.025	0.153 ± 0.028	0.792 $\pm 7.1\text{e-}03$	0.804 ± 0.012
NonInvasiveFetalECGThorax2	0.826 $\pm 2.6\text{e-}03$	0.798 $\pm 2.8\text{e-}04$	0.835 ± 0.011	0.852 $\pm 3.8\text{e-}03$	0.728 ± 0.016	0.823 ± 0.022	0.157 ± 0.034	0.826 $\pm 8.9\text{e-}03$	0.845 $\pm 8.5\text{e-}03$
OSULeaf	0.647 ± 0.012	0.618 ± 0.0	0.667 ± 0.033	0.715 ± 0.010	0.558 $\pm 8.1\text{e-}03$	0.666 ± 0.014	0.532 ± 0.045	0.673 ± 0.019	0.702 ± 0.030
Plane	0.988 $\pm 4.3\text{e-}03$	0.912 ± 0.0	0.934 ± 0.011	0.935 ± 0.023	0.917 ± 0.027	0.988 $\pm 9.6\text{e-}03$	0.842 ± 0.16	0.933 ± 0.030	0.965 ± 0.029
PowerCons	0.901 ± 0.018	0.897 ± 0.0	0.903 ± 0.018	0.911 ± 0.013	0.832 ± 0.024	0.907 ± 0.019	0.939 $\pm 8.2\text{e-}03$	0.904 ± 0.018	0.910 ± 0.028
RefrigerationDevices	0.531 $\pm 2.5\text{e-}03$	0.525 ± 0.0	0.504 ± 0.013	0.519 ± 0.034	0.485 ± 0.042	0.521 $\pm 7.4\text{e-}03$	0.485 ± 0.015	0.519 ± 0.035	0.486 ± 0.027
ScreenType	0.444 ± 0.010	0.389 ± 0.0	0.475 $\pm 2.2\text{e-}03$	0.481 ± 0.014	0.458 ± 0.026	0.507 ± 0.017	0.473 ± 0.033	0.455 ± 0.020	0.473 ± 0.030
SemgHandGenderCh2	0.904 $\pm 9.4\text{e-}03$	0.742 ± 0.0	0.811 $\pm 8.6\text{e-}03$	0.889 ± 0.014	0.822 ± 0.034	0.887 ± 0.012	0.865 $\pm 5.4\text{e-}03$	0.874 ± 0.019	0.904 $\pm 8.4\text{e-}03$
SemgHandMovementCh2	0.704 ± 0.016	0.427 ± 0.0	0.543 ± 0.014	0.664 ± 0.011	0.624 ± 0.022	0.748 ± 0.035	0.536 ± 0.022	0.658 ± 0.020	0.708 ± 0.023
SemgHandSubjectCh2	0.835 $\pm 6.6\text{e-}03$	0.618 ± 0.0	0.712 $\pm 5.2\text{e-}03$	0.836 ± 0.013	0.752 $\pm 8.4\text{e-}03$	0.813 ± 0.027	0.673 ± 0.015	0.806 ± 0.021	0.840 ± 0.013
ShapesAll	0.713 $\pm 6.7\text{e-}03$	0.688 $\pm 7.0\text{e-}04$	0.618 ± 0.012	0.654 ± 0.014	0.537 ± 0.018	0.685 ± 0.031	0.101 ± 0.017	0.583 ± 0.017	0.692 ± 0.011
SmallKitchenAppliances	0.749 $\pm 8.0\text{e-}03$	0.741 ± 0.0	0.798 $\pm 7.3\text{e-}03$	0.781 ± 0.011	0.757 ± 0.019	0.809 $\pm 7.7\text{e-}03$	0.781 ± 0.011	0.768 ± 0.022	0.777 ± 0.024
StarLightCurves	0.929 $\pm 7.5\text{e-}04$	0.885 $\pm 3.7\text{e-}05$	0.934 $\pm 1.2\text{e-}03$	0.941 $\pm 1.5\text{e-}03$	0.933 ± 0.012	0.943 $\pm 5.2\text{e-}03$	0.932 $\pm 7.4\text{e-}03$	0.927 $\pm 6.7\text{e-}03$	0.939 $\pm 4.4\text{e-}03$
Strawberry	0.910 $\pm 5.2\text{e-}03$	0.705 ± 0.0	0.862 $\pm 1.3\text{e-}03$	0.923 $\pm 5.1\text{e-}03$	0.864 ± 0.018	0.905 ± 0.010	0.870 $\pm 7.4\text{e-}03$	0.904 ± 0.011	0.906 ± 0.014
SwedishLeaf	0.823 ± 0.021	0.807 $\pm 1.4\text{e-}03$	0.838 $\pm 6.0\text{e-}03$	0.849 $\pm 6.7\text{e-}03$	0.785 ± 0.019	0.862 ± 0.021	0.559 ± 0.064	0.813 ± 0.016	0.857 ± 0.019
Trace	1.00 ± 0.0	0.913 ± 0.0	0.999 $\pm 4.2\text{e-}03$	1.00 ± 0.0	0.997 $\pm 9.8\text{e-}03$	0.967 ± 0.083	0.812 ± 0.12	0.996 $\pm 6.4\text{e-}03$	0.989 ± 0.018
TwoPatterns	0.765 $\pm 3.1\text{e-}03$	0.787 ± 0.0	0.805 $\pm 2.0\text{e-}03$	0.841 $\pm 7.1\text{e-}03$	0.831 $\pm 9.3\text{e-}03$	0.833 $\pm 4.9\text{e-}03$	0.746 $\pm 4.6\text{e-}03$	0.828 $\pm 7.7\text{e-}03$	0.852 $\pm 5.6\text{e-}03$
UWaveGestureLibraryAll	0.740 $\pm 6.3\text{e-}03$	0.667 ± 0.0	0.716 $\pm 2.4\text{e-}03$	0.768 $\pm 2.0\text{e-}03$	0.679 ± 0.012	0.793 ± 0.014	0.681 $\pm 9.9\text{e-}03$	0.716 ± 0.012	0.791 $\pm 7.2\text{e-}03$
UWaveGestureLibraryX	0.705 $\pm 9.4\text{e-}03$	0.662 $\pm 2.0\text{e-}03$	0.689 $\pm 3.0\text{e-}03$	0.718 ± 0.010	0.668 $\pm 6.9\text{e-}03$	0.735 $\pm 7.5\text{e-}03$	0.600 ± 0.019	0.678 ± 0.015	0.728 $\pm 4.9\text{e-}03$
UWaveGestureLibraryY	0.647 $\pm 4.3\text{e-}03$	0.538 $\pm 2.7\text{e-}03$	0.602 $\pm 1.9\text{e-}03$	0.651 $\pm 7.0\text{e-}03$	0.577 ± 0.015	0.682 $\pm 7.9\text{e-}03$	0.519 ± 0.017	0.600 ± 0.011	0.659 ± 0.010
UWaveGestureLibraryZ	0.660 $\pm 9.6\text{e-}03$	0.617 ± 0.0	0.643 $\pm 1.3\text{e-}03$	0.669 ± 0.011	0.604 $\pm 4.8\text{e-}03$	0.667 ± 0.012	0.592 ± 0.011	0.645 ± 0.015	0.674 $\pm 5.7\text{e-}03$
Wafer	0.961 $\pm 8.3\text{e-}04$	0.969 ± 0.0	0.974 $\pm 3.3\text{e-}03$	0.978 $\pm 1.5\text{e-}03$	0.970 $\pm 9.6\text{e-}03$	0.986 $\pm 6.3\text{e-}03$	0.988 $\pm 6.6\text{e-}03$	0.974 $\pm 4.1\text{e-}03$	0.987 $\pm 5.4\text{e-}03$
Worms	0.712 ± 0.044	0.635 ± 0.0	0.641 ± 0.037	0.675 ± 0.018	0.532 ± 0.039	0.639 ± 0.033	0.471 ± 0.056	0.592 ± 0.047	0.627 ± 0.055
WormsTwoClass	0.855 ± 0.023	0.818 ± 0.0	0.764 $\pm 7.2\text{e-}03$	0.766 ± 0.036	0.740 ± 0.019	0.841 ± 0.023	0.722 ± 0.032	0.703 ± 0.053	0.791 ± 0.046
Yoga	0.739 $\pm 3.3\text{e-}04$	0.582 ± 0.0	0.673 $\pm 3.7\text{e-}03$	0.725 ± 0.013	0.699 ± 0.018	0.732 ± 0.015	0.705 $\pm 8.7\text{e-}03$	0.694 ± 0.016	0.721 ± 0.023

Table 8: Geometric mean of inference OPs for Catch22 across 10 random seeds assuming FP16 for floating-point and INT16 for integer arithmetic.

	KNN	NB	LR	SVM	DT	RF	AB	MLP	DLN
ACSF1	1.15M	2.52M	1.81M	8.20M	915	115K	190K	8.13M	31.9K
ChlorineConcentration	7.85M	679K	518K	29.8M	1.65K	176K	222K	7.53M	38.6K
Computers	1.64M	445K	171K	10.7M	695	137K	205K	2.52M	26.5K
CricketX	2.69M	2.71M	2.07M	63.1M	1.23K	186K	252K	4.66M	85.2K
CricketY	2.69M	2.71M	2.07M	49.1M	1.34K	193K	239K	5.43M	67.8K
CricketZ	2.69M	2.71M	2.07M	52.5M	1.74K	170K	240K	6.81M	68.8K
Earthquakes	4.59M	452K	173K	16.9M	512	25.9K	234K	4.37M	13.6K
EOGHorizontalSignal	2.49M	2.71M	2.07M	38.9M	1.50K	161K	251K	4.57M	58.2K
EOGVerticalSignal	2.49M	2.71M	2.07M	32.2M	1.35K	192K	262K	7.22M	55.0K
EthanolLevel	5.29M	860K	676K	39.7M	952	152K	186K	2.40M	32.6K
FaceAll	3.92M	3.17M	2.42M	71.8M	1.52K	178K	271K	4.63M	76.4K
Fish	1.04M	1.51M	1.18M	12.2M	878	177K	224K	3.00M	49.2K
FordA	27.0M	452K	173K	85.6M	1.34K	163K	255K	1.47M	27.7K
FordB	27.3M	452K	173K	79.2M	1.41K	175K	261K	1.81M	30.1K
FreezerRegularTrain	1.95M	475K	176K	932K	183	12.6K	136K	6.54M	7.57K
GunPointAgeSpan	962K	467K	175K	5.64M	750	120K	200K	4.47M	47.1K
GunPointMaleVersusFemale	962K	467K	175K	2.26M	348	56.3K	176K	4.38M	10.8K
GunPointOldVersusYoung	1.29M	460K	174K	3.31M	183	20.7K	136K	5.14M	8.39K
Ham	1.25M	452K	173K	3.01M	988	86.4K	143K	4.03M	25.3K
HandOutlines	8.54M	430K	169K	29.6M	1.48K	148K	242K	2.46M	33.8K
Haptics	1.03M	1.13M	863K	15.1M	878	130K	181K	2.89M	37.8K
InlineSkate	672K	1.61M	1.22M	3.35M	1.02K	147K	219K	3.81M	31.9K
InsectWingbeatSound	1.49M	2.49M	1.90M	23.8M	878	87.8K	232K	6.13M	40.9K
LargeKitchenAppliances	2.59M	679K	518K	7.17M	1.10K	174K	248K	3.66M	34.7K
MixedShapesRegularTrain	3.36M	1.11M	857K	37.1M	1.17K	184K	191K	5.83M	36.5K
MixedShapesSmallTrain	630K	1.11M	857K	5.40M	677	86.9K	170K	3.47M	31.1K
NonInvasiveFetalECGThorax1	13.2M	9.50M	7.25M	102M	1.85K	152K	245K	5.25M	185K
NonInvasiveFetalECGThorax2	13.2M	9.50M	7.25M	93.4M	1.90K	139K	240K	5.44M	160K
OSULeaf	2.33M	1.36M	1.04M	26.0M	988	132K	136K	4.30M	46.4K
Plane	689K	1.58M	1.21M	4.41M	824	107K	221K	4.68M	27.3K
PowerCons	964K	452K	173K	7.97M	366	96.4K	177K	4.40M	52.8K
RefrigerationDevices	2.59M	679K	518K	42.2M	1.63K	165K	160K	7.74M	39.9K
ScreenType	2.49M	668K	514K	22.4M	1.45K	116K	217K	3.09M	37.3K
SemgHandGenderCh2	2.05M	452K	173K	18.1M	1.24K	123K	236K	4.33M	34.0K
SemgHandMovementCh2	3.13M	1.36M	1.04M	60.2M	1.90K	176K	237K	5.67M	53.9K
SemgHandSubjectCh2	3.13M	1.13M	863K	54.2M	1.56K	157K	164K	4.82M	40.4K
ShapesAll	4.21M	13.6M	10.4M	77.1M	1.63K	164K	247K	10.4M	203K
SmallKitchenAppliances	2.59M	679K	518K	28.0M	622	144K	208K	4.13M	39.2K
StarLightCurves	6.91M	668K	514K	6.11M	714	103K	213K	1.94M	39.3K
Strawberry	4.76M	475K	176K	26.6M	1.43K	184K	257K	5.86M	27.8K
SwedishLeaf	3.49M	3.39M	2.59M	32.9M	1.28K	175K	263K	4.57M	65.5K
Trace	937K	920K	696K	3.83M	439	42.5K	204K	5.05M	9.25K
TwoPatterns	7.16M	905K	691K	59.6M	1.59K	180K	216K	2.79M	32.5K
UWaveGestureLibraryAll	6.39M	1.81M	1.38M	78.8M	1.67K	169K	270K	4.94M	71.7K
UWaveGestureLibraryX	6.39M	1.81M	1.38M	69.2M	1.15K	178K	257K	3.53M	61.6K
UWaveGestureLibraryY	6.39M	1.81M	1.38M	112M	1.37K	181K	234K	7.52M	65.6K
UWaveGestureLibraryZ	5.50M	1.69M	1.34M	46.0M	1.54K	146K	228K	2.89M	47.9K
Wafer	7.16M	452K	173K	15.3M	805	79.0K	199K	4.08M	20.0K
Worms	2.22M	1.13M	863K	8.53M	586	79.1K	178K	4.67M	30.7K
WormsTwoClass	1.05M	452K	173K	11.2M	952	125K	205K	3.33M	31.6K
Yoga	2.20M	467K	175K	29.0M	1.12K	129K	211K	7.98M	26.2K

Table 9: Best-of-10 test balanced accuracy for TSFresh-10.

	KNN	NB	LR	SVM	DT	RF	AB	MLP	DLN
ACSF1	0.780	0.690	0.640	0.750	0.670	0.810	0.610	0.730	0.780
ChlorineConcentration	0.647	0.431	0.448	0.709	0.552	0.531	0.462	0.655	0.549
Computers	0.680	0.668	0.708	0.676	0.656	0.692	0.664	0.652	0.700
CricketX	0.559	0.417	0.511	0.577	0.416	0.545	0.358	0.522	0.522
CricketY	0.594	0.481	0.557	0.627	0.480	0.602	0.419	0.577	0.576
CricketZ	0.579	0.472	0.515	0.569	0.443	0.530	0.402	0.506	0.531
Earthquakes	0.585	0.656	0.646	0.674	0.636	0.660	0.595	0.646	0.632
EOGHorizontalSignal	0.442	0.447	0.517	0.471	0.464	0.561	0.358	0.508	0.471
EOGVerticalSignal	0.420	0.361	0.422	0.384	0.378	0.434	0.410	0.425	0.396
EthanolLevel	0.326	0.343	0.364	0.364	0.343	0.382	0.380	0.369	0.368
FaceAll	0.722	0.659	0.691	0.739	0.607	0.724	0.552	0.706	0.728
Fish	0.838	0.838	0.840	0.849	0.730	0.818	0.699	0.814	0.838
FordA	1.00	1.00	1.00	1.00	1.00	1.00	1.00	1.00	1.00
FordB	0.738	0.732	0.773	0.793	0.731	0.754	0.750	0.787	0.753
FreezerRegularTrain	0.906	0.891	0.944	0.942	0.941	0.958	0.946	0.942	0.944
GunPointAgeSpan	0.965	0.880	0.915	0.965	0.927	0.953	0.943	0.978	0.972
GunPointMaleVersusFemale	0.948	0.780	0.967	0.978	0.978	0.994	0.985	0.991	0.994
GunPointOldVersusYoung	0.997	1.00	1.00	1.00	1.00	1.00	1.00	1.00	1.00
Ham	0.705	0.727	0.717	0.747	0.708	0.744	0.705	0.690	0.678
HandOutlines	0.825	0.614	0.764	0.869	0.838	0.860	0.815	0.863	0.872
Haptics	0.416	0.413	0.454	0.446	0.403	0.466	0.393	0.431	0.454
InlineSkate	0.425	0.341	0.317	0.416	0.349	0.376	0.280	0.355	0.441
InsectWingbeatSound	0.583	0.568	0.581	0.571	0.454	0.581	0.481	0.539	0.546
LargeKitchenAppliances	0.755	0.579	0.672	0.749	0.728	0.784	0.771	0.779	0.760
MixedShapesRegularTrain	0.935	0.879	0.911	0.936	0.884	0.917	0.859	0.917	0.930
MixedShapesSmallTrain	0.835	0.845	0.848	0.862	0.757	0.848	0.777	0.833	0.835
NonInvasiveFetalECGThorax1	0.787	0.775	0.813	0.847	0.681	0.795	0.227	0.816	0.787
NonInvasiveFetalECGThorax2	0.835	0.833	0.853	0.883	0.751	0.827	0.263	0.827	0.811
OSULeaf	0.871	0.882	0.917	0.901	0.803	0.868	0.697	0.861	0.873
Plane	0.943	0.959	0.977	0.980	0.904	0.973	0.808	0.956	0.980
PowerCons	0.876	0.808	0.869	0.876	0.813	0.841	0.855	0.890	0.876
RefrigerationDevices	0.605	0.477	0.605	0.619	0.584	0.632	0.600	0.613	0.611
ScreenType	0.467	0.392	0.448	0.456	0.515	0.541	0.536	0.453	0.493
SemgHandGenderCh2	0.795	0.676	0.799	0.843	0.823	0.852	0.832	0.817	0.842
SemgHandMovementCh2	0.873	0.407	0.587	0.873	0.736	0.804	0.469	0.831	0.811
SemgHandSubjectCh2	0.916	0.660	0.791	0.918	0.842	0.880	0.800	0.900	0.904
ShapesAll	0.757	0.703	0.737	0.757	0.608	0.720	0.107	0.707	0.745
SmallKitchenAppliances	0.677	0.611	0.672	0.723	0.725	0.755	0.691	0.720	0.725
StarLightCurves	0.956	0.899	0.946	0.961	0.950	0.955	0.954	0.958	0.957
Strawberry	0.953	0.844	0.840	0.946	0.934	0.941	0.939	0.950	0.933
SwedishLeaf	0.871	0.823	0.892	0.901	0.810	0.871	0.609	0.890	0.880
Trace	0.791	0.867	0.930	0.934	0.867	0.881	0.750	0.880	0.894
TwoPatterns	0.999	0.963	0.999	0.999	0.980	0.995	0.747	0.999	0.998
UWaveGestureLibraryAll	0.952	0.928	0.921	0.961	0.884	0.950	0.885	0.936	0.947
UWaveGestureLibraryX	0.780	0.717	0.754	0.800	0.702	0.780	0.694	0.764	0.768
UWaveGestureLibraryY	0.685	0.593	0.667	0.716	0.625	0.686	0.547	0.679	0.666
UWaveGestureLibraryZ	0.711	0.648	0.708	0.726	0.651	0.714	0.620	0.714	0.705
Wafer	1.00	0.992	1.00	1.00	0.995	1.00	0.995	1.00	1.00
Worms	0.521	0.449	0.479	0.551	0.489	0.520	0.486	0.601	0.568
WormsTwoClass	0.803	0.777	0.750	0.826	0.746	0.795	0.818	0.864	0.803
Yoga	0.897	0.865	0.905	0.910	0.882	0.904	0.896	0.906	0.900

Table 10: Mean and standard deviation of balanced accuracy for TSFresh-10 across 10 random seeds.

	KNN	NB	LR	SVM	DT	RF	AB	MLP	DLN
ACSF1	0.739 ± 0.033	0.690 ± 0.0	0.618 ± 0.019	0.708 ± 0.034	0.597 ± 0.058	0.732 ± 0.058	0.525 ± 0.047	0.694 ± 0.027	0.723 ± 0.047
ChlorineConcentration	0.637 ± 0.021	0.431 ± 0.0	0.446 ± 2.3e-03	0.697 ± 0.011	0.482 ± 0.044	0.514 ± 0.013	0.451 ± 9.9e-03	0.618 ± 0.028	0.526 ± 0.014
Computers	0.649 ± 0.038	0.668 ± 0.0	0.693 ± 6.3e-03	0.658 ± 0.017	0.608 ± 0.035	0.673 ± 0.013	0.648 ± 7.9e-03	0.637 ± 0.014	0.654 ± 0.024
CricketX	0.547 ± 0.012	0.417 ± 0.0	0.507 ± 2.2e-03	0.563 ± 8.9e-03	0.385 ± 0.014	0.533 ± 8.0e-03	0.330 ± 0.017	0.500 ± 0.013	0.489 ± 0.016
CricketY	0.584 ± 0.011	0.481 ± 0.0	0.556 ± 4.4e-03	0.613 ± 0.016	0.458 ± 0.025	0.577 ± 0.014	0.395 ± 0.014	0.539 ± 0.027	0.546 ± 0.028
CricketZ	0.562 ± 0.013	0.472 ± 0.0	0.508 ± 7.1e-03	0.549 ± 0.019	0.435 ± 9.9e-03	0.509 ± 0.019	0.370 ± 0.019	0.483 ± 0.020	0.503 ± 0.018
EOGHorizontalSignal	0.428 ± 0.014	0.447 ± 0.0	0.505 ± 8.5e-03	0.446 ± 0.014	0.442 ± 0.019	0.503 ± 0.025	0.323 ± 0.028	0.434 ± 0.044	0.428 ± 0.026
EOGVerticalSignal	0.401 ± 0.016	0.361 ± 0.0	0.411 ± 6.7e-03	0.357 ± 0.020	0.349 ± 0.018	0.419 ± 0.013	0.343 ± 0.042	0.366 ± 0.034	0.379 ± 0.012
Earthquakes	0.557 ± 0.033	0.656 ± 0.0	0.622 ± 0.018	0.637 ± 0.019	0.603 ± 0.043	0.647 ± 8.4e-03	0.584 ± 6.8e-03	0.584 ± 0.037	0.594 ± 0.020
EthanolLevel	0.307 ± 0.012	0.343 ± 0.0	0.362 ± 2.8e-03	0.356 ± 9.2e-03	0.316 ± 0.022	0.363 ± 0.012	0.363 ± 0.013	0.334 ± 0.021	0.351 ± 0.014
FaceAll	0.718 ± 4.7e-03	0.659 ± 0.0	0.684 ± 4.3e-03	0.729 ± 0.013	0.580 ± 0.015	0.707 ± 0.010	0.498 ± 0.027	0.687 ± 0.013	0.716 ± 0.010
Fish	0.819 ± 0.019	0.838 ± 0.0	0.819 ± 0.023	0.831 ± 0.012	0.688 ± 0.032	0.784 ± 0.032	0.658 ± 0.029	0.772 ± 0.031	0.792 ± 0.032
FordA	1.00 ± 0.0	1.00 ± 0.0	1.00 ± 0.0	1.00 ± 0.0	1.00 ± 0.0	1.00 ± 0.0	1.00 ± 0.0	1.00 ± 0.0	1.00 ± 0.0
FordB	0.728 ± 6.6e-03	0.732 ± 0.0	0.771 ± 1.1e-03	0.785 ± 7.1e-03	0.724 ± 7.7e-03	0.748 ± 3.7e-03	0.745 ± 4.6e-03	0.773 ± 9.6e-03	0.744 ± 6.0e-03
FreezerRegularTrain	0.901 ± 4.7e-03	0.891 ± 0.0	0.934 ± 5.1e-03	0.940 ± 2.0e-03	0.921 ± 6.9e-03	0.936 ± 0.016	0.929 ± 8.4e-03	0.933 ± 5.7e-03	0.936 ± 5.2e-03
GunPointAgeSpan	0.952 ± 0.018	0.880 ± 0.0	0.892 ± 0.017	0.943 ± 0.025	0.909 ± 0.014	0.943 ± 4.9e-03	0.935 ± 7.4e-03	0.965 ± 9.1e-03	0.957 ± 0.012
GunPointMaleVersusFemale	0.942 ± 0.011	0.780 ± 0.0	0.960 ± 3.7e-03	0.970 ± 5.4e-03	0.978 ± 0.0	0.988 ± 2.7e-03	0.985 ± 0.0	0.978 ± 8.8e-03	0.973 ± 0.015
GunPointOldVersusYoung	0.997 ± 0.0	1.00 ± 0.0	1.00 ± 0.0	1.00 ± 0.0	1.00 ± 0.0	1.00 ± 0.0	1.00 ± 1.1e-03	1.00 ± 0.0	0.999 ± 1.6e-03
Ham	0.666 ± 0.029	0.727 ± 0.0	0.682 ± 0.022	0.662 ± 0.041	0.645 ± 0.057	0.700 ± 0.035	0.658 ± 0.032	0.603 ± 0.058	0.621 ± 0.036
HandOutlines	0.825 ± 0.0	0.614 ± 0.0	0.764 ± 0.0	0.853 ± 0.012	0.822 ± 0.010	0.849 ± 6.3e-03	0.811 ± 4.5e-03	0.850 ± 9.6e-03	0.854 ± 0.015
Haptics	0.406 ± 9.2e-03	0.413 ± 0.0	0.431 ± 0.018	0.417 ± 0.027	0.375 ± 0.020	0.445 ± 0.018	0.372 ± 0.015	0.406 ± 0.024	0.415 ± 0.023
InlineSkate	0.413 ± 0.012	0.341 ± 0.0	0.304 ± 7.3e-03	0.364 ± 0.034	0.325 ± 0.019	0.352 ± 0.018	0.245 ± 0.019	0.332 ± 0.024	0.404 ± 0.022
InsectWingbeatSound	0.572 ± 0.013	0.568 ± 0.0	0.555 ± 0.026	0.550 ± 0.015	0.442 ± 0.013	0.568 ± 6.7e-03	0.445 ± 0.027	0.514 ± 0.015	0.528 ± 0.016
LargeKitchenAppliances	0.747 ± 7.2e-03	0.579 ± 0.0	0.664 ± 5.6e-03	0.723 ± 0.020	0.700 ± 0.021	0.766 ± 9.9e-03	0.753 ± 0.014	0.730 ± 0.029	0.743 ± 0.013
MixedShapesRegularTrain	0.931 ± 3.1e-03	0.879 ± 0.0	0.909 ± 6.3e-04	0.930 ± 4.4e-03	0.873 ± 5.5e-03	0.911 ± 3.5e-03	0.843 ± 0.011	0.913 ± 5.0e-03	0.918 ± 6.7e-03

continued on next page

Table 10 (continued)

	KNN	NB	LR	SVM	DT	RF	AB	MLP	DLN
MixedShapesSmallTrain	0.830 $\pm 2.9\text{e-}03$	0.845 ± 0.0	0.827 ± 0.018	0.847 $\pm 7.3\text{e-}03$	0.728 ± 0.021	0.842 $\pm 5.3\text{e-}03$	0.746 ± 0.017	0.816 ± 0.028	0.820 ± 0.012
NonInvasiveFetalECGThorax1	0.781 $\pm 3.3\text{e-}03$	0.775 ± 0.0	0.809 $\pm 1.3\text{e-}03$	0.837 $\pm 5.2\text{e-}03$	0.666 $\pm 8.1\text{e-}03$	0.767 ± 0.025	0.172 ± 0.031	0.804 ± 0.010	0.766 ± 0.016
NonInvasiveFetalECGThorax2	0.833 $\pm 2.1\text{e-}03$	0.833 ± 0.0	0.840 $\pm 8.8\text{e-}03$	0.875 $\pm 5.5\text{e-}03$	0.740 ± 0.012	0.806 ± 0.025	0.161 ± 0.053	0.815 $\pm 9.8\text{e-}03$	0.792 ± 0.017
OSULeaf	0.863 $\pm 6.7\text{e-}03$	0.882 ± 0.0	0.879 ± 0.043	0.894 $\pm 5.7\text{e-}03$	0.788 $\pm 6.1\text{e-}03$	0.852 ± 0.011	0.635 ± 0.033	0.833 ± 0.025	0.845 ± 0.019
Plane	0.923 ± 0.016	0.959 ± 0.0	0.943 ± 0.039	0.970 $\pm 5.0\text{e-}03$	0.890 ± 0.013	0.950 ± 0.015	0.674 ± 0.15	0.926 ± 0.021	0.960 ± 0.022
PowerCons	0.849 ± 0.026	0.808 ± 0.0	0.863 $\pm 7.8\text{e-}03$	0.867 $\pm 5.8\text{e-}03$	0.812 $\pm 4.3\text{e-}03$	0.815 ± 0.013	0.828 ± 0.016	0.862 ± 0.024	0.837 ± 0.021
RefrigerationDevices	0.585 ± 0.021	0.477 ± 0.0	0.596 ± 0.014	0.591 ± 0.028	0.541 ± 0.023	0.609 ± 0.011	0.566 ± 0.023	0.580 ± 0.021	0.579 ± 0.020
ScreenType	0.448 ± 0.017	0.392 ± 0.0	0.442 $\pm 2.8\text{e-}03$	0.417 ± 0.023	0.483 ± 0.029	0.532 $\pm 8.5\text{e-}03$	0.507 ± 0.021	0.412 ± 0.023	0.459 ± 0.026
SemgHandGenderCh2	0.789 $\pm 6.6\text{e-}03$	0.676 ± 0.0	0.774 ± 0.022	0.835 $\pm 8.8\text{e-}03$	0.796 ± 0.022	0.840 $\pm 9.1\text{e-}03$	0.823 $\pm 8.7\text{e-}03$	0.785 ± 0.014	0.827 ± 0.012
SemgHandMovementCh2	0.853 ± 0.017	0.407 ± 0.0	0.565 ± 0.010	0.849 ± 0.021	0.684 ± 0.025	0.779 ± 0.038	0.442 ± 0.020	0.797 ± 0.020	0.776 ± 0.017
SemgHandSubjectCh2	0.905 $\pm 5.8\text{e-}03$	0.660 ± 0.0	0.787 $\pm 1.8\text{e-}03$	0.898 ± 0.023	0.822 ± 0.017	0.869 $\pm 7.6\text{e-}03$	0.778 ± 0.013	0.865 ± 0.015	0.882 ± 0.016
ShapesAll	0.753 $\pm 2.7\text{e-}03$	0.703 ± 0.0	0.727 $\pm 7.4\text{e-}03$	0.739 $\pm 7.0\text{e-}03$	0.580 ± 0.017	0.678 ± 0.049	0.0915 ± 0.013	0.688 ± 0.013	0.692 ± 0.036
SmallKitchenAppliances	0.659 ± 0.015	0.611 ± 0.0	0.670 $\pm 1.1\text{e-}03$	0.704 ± 0.020	0.706 ± 0.015	0.737 $\pm 9.3\text{e-}03$	0.667 ± 0.014	0.687 ± 0.028	0.697 ± 0.014
StarLightCurves	0.955 $\pm 9.3\text{e-}04$	0.899 ± 0.0	0.944 $\pm 2.2\text{e-}03$	0.957 $\pm 2.4\text{e-}03$	0.949 $\pm 1.0\text{e-}03$	0.923 ± 0.093	0.949 $\pm 3.3\text{e-}03$	0.953 $\pm 5.6\text{e-}03$	0.954 $\pm 2.6\text{e-}03$
Strawberry	0.946 $\pm 3.7\text{e-}03$	0.844 ± 0.0	0.835 $\pm 3.0\text{e-}03$	0.937 $\pm 5.6\text{e-}03$	0.920 ± 0.011	0.930 $\pm 8.0\text{e-}03$	0.921 ± 0.014	0.927 ± 0.012	0.926 $\pm 5.7\text{e-}03$
SwedishLeaf	0.862 $\pm 4.5\text{e-}03$	0.823 ± 0.0	0.890 $\pm 1.1\text{e-}03$	0.896 $\pm 3.9\text{e-}03$	0.778 ± 0.016	0.855 ± 0.016	0.490 ± 0.079	0.877 $\pm 8.2\text{e-}03$	0.860 ± 0.013
Trace	0.777 ± 0.013	0.867 ± 0.0	0.918 ± 0.010	0.918 ± 0.012	0.858 ± 0.011	0.854 ± 0.018	0.750 ± 0.0	0.859 ± 0.016	0.876 ± 0.017
TwoPatterns	0.998 $\pm 4.0\text{e-}04$	0.963 ± 0.0	0.996 $\pm 3.2\text{e-}03$	0.999 $\pm 5.4\text{e-}04$	0.978 $\pm 1.5\text{e-}03$	0.992 $\pm 2.1\text{e-}03$	0.746 $\pm 9.9\text{e-}04$	0.997 $\pm 1.7\text{e-}03$	0.996 $\pm 9.4\text{e-}04$
UWaveGestureLibraryAll	0.947 $\pm 2.2\text{e-}03$	0.928 ± 0.0	0.919 $\pm 2.7\text{e-}03$	0.957 $\pm 8.6\text{e-}03$	0.874 $\pm 7.7\text{e-}03$	0.937 $\pm 9.9\text{e-}03$	0.871 $\pm 8.2\text{e-}03$	0.929 $\pm 5.4\text{e-}03$	0.939 $\pm 5.6\text{e-}03$
UWaveGestureLibraryX	0.774 $\pm 3.7\text{e-}03$	0.717 ± 0.0	0.751 $\pm 2.5\text{e-}03$	0.787 $\pm 6.9\text{e-}03$	0.695 $\pm 5.4\text{e-}03$	0.769 $\pm 9.2\text{e-}03$	0.683 ± 0.010	0.743 ± 0.014	0.760 $\pm 8.2\text{e-}03$
UWaveGestureLibraryY	0.680 $\pm 3.3\text{e-}03$	0.593 ± 0.0	0.665 $\pm 7.6\text{e-}04$	0.705 $\pm 7.5\text{e-}03$	0.605 ± 0.012	0.682 $\pm 5.1\text{e-}03$	0.535 $\pm 8.3\text{e-}03$	0.669 $\pm 6.0\text{e-}03$	0.655 $\pm 8.7\text{e-}03$
UWaveGestureLibraryZ	0.706 $\pm 6.0\text{e-}03$	0.648 ± 0.0	0.703 $\pm 7.4\text{e-}03$	0.721 $\pm 5.6\text{e-}03$	0.640 $\pm 7.4\text{e-}03$	0.704 ± 0.011	0.606 ± 0.010	0.701 ± 0.010	0.690 ± 0.011
Wafer	1.00 ± 0.0	0.992 ± 0.0	1.00 ± 0.0	1.00 ± 0.0	0.993 $\pm 1.3\text{e-}03$	0.999 $\pm 1.7\text{e-}03$	0.995 $\pm 1.3\text{e-}03$	1.00 ± 0.0	0.997 $\pm 5.2\text{e-}03$
Worms	0.484 ± 0.077	0.449 ± 0.0	0.457 ± 0.017	0.526 ± 0.016	0.405 ± 0.049	0.442 ± 0.034	0.428 ± 0.037	0.501 ± 0.046	0.440 ± 0.11
WormsTwoClass	0.776 ± 0.018	0.777 ± 0.0	0.740 $\pm 3.6\text{e-}03$	0.782 ± 0.032	0.718 ± 0.025	0.764 ± 0.031	0.771 ± 0.024	0.761 ± 0.051	0.756 ± 0.039
Yoga	0.893 $\pm 3.3\text{e-}03$	0.865 ± 0.0	0.905 $\pm 4.5\text{e-}04$	0.906 $\pm 2.1\text{e-}03$	0.865 ± 0.012	0.902 $\pm 1.4\text{e-}03$	0.890 $\pm 3.2\text{e-}03$	0.896 ± 0.010	0.890 ± 0.012

Table 11: Geometric mean of inference OPs for TSFresh-10 across 10 random seeds assuming FP16 for floating-point and INT16 for integer arithmetic.

	KNN	NB	LR	SVM	DT	RF	AB	MLP	DLN
ACSF1	1.14M	1.82M	1.58M	8.21M	1.13K	132K	219K	1.26M	24.2K
ChlorineConcentration	6.57M	544K	473K	43.2M	1.56K	170K	247K	2.26M	25.7K
Computers	1.79M	363K	158K	23.5M	714	95.9K	158K	792K	10.8K
CricketX	2.84M	2.18M	1.89M	50.4M	1.56K	170K	229K	1.60M	38.9K
CricketY	1.97M	2.18M	1.89M	48.1M	1.54K	152K	222K	1.46M	39.4K
CricketZ	1.97M	2.18M	1.89M	51.1M	1.56K	180K	256K	1.43M	33.6K
Earthquakes	4.13M	363K	158K	15.0M	549	33.2K	227K	740K	4.91K
EOGHorizontalSignal	1.42M	2.18M	1.89M	36.5M	1.30K	163K	239K	1.73M	39.1K
EOGVerticalSignal	3.44M	2.18M	1.89M	39.0M	1.39K	214K	248K	1.45M	33.1K
EthanolLevel	5.40M	726K	631K	36.7M	1.02K	151K	232K	783K	14.8K
FaceAll	2.25M	2.54M	2.21M	48.2M	1.52K	173K	274K	1.44M	46.0K
Fish	2.41M	1.27M	1.10M	17.7M	1.24K	167K	221K	1.25M	22.2K
FordA	20.3M	363K	158K	24.7M	183	21.8K	136K	1.05M	1.55K
FordB	15.5M	356K	156K	30.0M	1.13K	187K	265K	304K	24.8K
FreezerRegularTrain	2.23M	363K	158K	1.93M	238	37.5K	191K	977K	7.96K
GunPointAgeSpan	795K	363K	158K	4.25M	531	81.5K	174K	1.18M	19.1K
GunPointMaleVersusFemale	526K	370K	159K	300K	549	93.4K	179K	868K	8.49K
GunPointOldVersusYoung	747K	378K	160K	1.45M	183	23.9K	136K	1.48M	1.57K
Ham	1.12M	363K	158K	3.81M	586	92.5K	170K	910K	13.7K
HandOutlines	9.78M	363K	158K	47.3M	1.63K	189K	235K	715K	23.3K
Haptics	745K	908K	789K	11.2M	878	92.3K	187K	1.59M	17.3K
InlineSkate	464K	1.27M	1.10M	6.26M	952	75.9K	157K	1.52M	17.0K
InsectWingbeatSound	1.08M	2.00M	1.74M	10.9M	1.32K	135K	248K	1.24M	29.0K
LargeKitchenAppliances	1.47M	544K	473K	23.8M	1.19K	143K	227K	1.78M	19.0K
MixedShapesRegularTrain	6.48M	908K	789K	30.8M	1.26K	176K	205K	1.06M	22.8K
MixedShapesSmallTrain	469K	908K	789K	7.59M	732	93.5K	212K	1.12M	16.4K
NonInvasiveFetalECGThorax1	23.9M	7.62M	6.62M	180M	1.96K	159K	261K	2.12M	98.9K
NonInvasiveFetalECGThorax2	7.80M	7.62M	6.62M	153M	1.99K	164K	270K	2.16M	76.3K
OSULeaf	975K	1.09M	946K	14.2M	695	121K	132K	1.41M	22.1K
Plane	494K	1.27M	1.10M	1.20M	1.04K	99.7K	192K	1.01M	14.5K
PowerCons	568K	370K	159K	2.88M	238	51.4K	200K	664K	6.50K
RefrigerationDevices	1.47M	544K	473K	17.2M	1.35K	162K	140K	1.02M	22.8K
ScreenType	1.47M	544K	473K	24.7M	1.04K	165K	219K	861K	18.5K
SemgHandGenderCh2	1.83M	363K	158K	19.4M	878	128K	199K	1.36M	14.2K
SemgHandMovementCh2	1.79M	1.09M	946K	42.5M	1.78K	151K	252K	2.70M	27.6K
SemgHandSubjectCh2	2.79M	908K	789K	34.3M	1.41K	184K	180K	1.41M	28.2K
ShapesAll	2.43M	10.9M	9.46M	55.4M	1.68K	184K	240K	2.54M	118K
SmallKitchenAppliances	3.15M	544K	473K	33.1M	1.21K	141K	178K	1.21M	19.2K
StarLightCurves	9.78M	544K	473K	13.7M	549	123K	174K	591K	7.71K
Strawberry	5.92M	363K	158K	21.1M	1.12K	129K	251K	1.22M	18.7K
SwedishLeaf	7.04M	2.72M	2.37M	15.5M	1.39K	135K	265K	1.48M	44.4K
Trace	635K	711K	626K	1.49M	512	65.9K	220K	748K	8.12K
TwoPatterns	5.30M	726K	631K	5.18M	1.37K	159K	193K	933K	23.6K
UWaveGestureLibraryAll	10.7M	1.45M	1.26M	63.7M	1.39K	154K	247K	1.95M	27.0K
UWaveGestureLibraryX	6.73M	1.45M	1.26M	59.4M	1.74K	168K	210K	1.36M	33.8K
UWaveGestureLibraryY	8.74M	1.45M	1.26M	79.5M	1.54K	186K	195K	1.64M	30.9K
UWaveGestureLibraryZ	11.7M	1.45M	1.26M	59.2M	1.88K	191K	227K	1.34M	30.8K
Wafer	5.30M	363K	158K	8.31M	183	24.5K	136K	1.05M	2.60K
Worms	1.47M	908K	789K	13.8M	695	50.0K	215K	779K	9.47K
WormsTwoClass	1.02M	356K	156K	8.47M	933	76.0K	188K	744K	35.5K
Yoga	1.60M	370K	159K	3.82M	805	132K	157K	1.22M	6.91K

Table 12: Best-of-10 test balanced accuracy for TSFresh-20.

	KNN	NB	LR	SVM	DT	RF	AB	MLP	DLN
ACSF1	0.790	0.720	0.750	0.800	0.660	0.860	0.690	0.780	0.800
ChlorineConcentration	0.664	0.423	0.475	0.749	0.574	0.581	0.467	0.682	0.599
Computers	0.652	0.576	0.700	0.676	0.608	0.712	0.728	0.644	0.708
CricketX	0.654	0.542	0.594	0.671	0.463	0.647	0.465	0.626	0.594
CricketY	0.670	0.531	0.633	0.690	0.534	0.648	0.444	0.631	0.647
CricketZ	0.655	0.567	0.581	0.664	0.491	0.590	0.452	0.605	0.606
Earthquakes	0.580	0.650	0.679	0.674	0.636	0.650	0.595	0.685	0.660
EOGHorizontalSignal	0.459	0.478	0.499	0.490	0.512	0.542	0.348	0.515	0.503
EOGVerticalSignal	0.439	0.391	0.461	0.485	0.457	0.501	0.456	0.477	0.482
EthanolLevel	0.372	0.414	0.468	0.426	0.366	0.415	0.373	0.446	0.442
FaceAll	0.817	0.707	0.784	0.835	0.648	0.790	0.598	0.791	0.792
Fish	0.892	0.855	0.866	0.884	0.733	0.885	0.753	0.880	0.883
FordA	1.00	1.00	1.00	1.00	1.00	1.00	1.00	1.00	1.00
FordB	0.791	0.699	0.789	0.814	0.752	0.794	0.773	0.788	0.796
FreezerRegularTrain	0.902	0.890	0.939	0.943	0.919	0.970	0.964	0.940	0.945
GunPointAgeSpan	0.984	0.915	0.949	0.949	0.940	0.969	0.956	0.975	0.978
GunPointMaleVersusFemale	0.990	0.973	0.991	0.994	0.965	0.972	0.972	0.997	1.00
GunPointOldVersusYoung	1.00	1.00	1.00	1.00	1.00	1.00	1.00	1.00	1.00
Ham	0.692	0.722	0.667	0.667	0.693	0.725	0.668	0.630	0.681
HandOutlines	0.861	0.781	0.833	0.866	0.867	0.904	0.861	0.870	0.889
Haptics	0.419	0.365	0.441	0.502	0.412	0.480	0.390	0.465	0.480
InlineSkate	0.394	0.327	0.339	0.362	0.358	0.426	0.281	0.372	0.434
InsectWingbeatSound	0.617	0.593	0.602	0.612	0.509	0.639	0.513	0.571	0.595
LargeKitchenAppliances	0.853	0.672	0.805	0.867	0.829	0.891	0.837	0.875	0.864
MixedShapesRegularTrain	0.922	0.886	0.926	0.943	0.880	0.925	0.881	0.931	0.941
MixedShapesSmallTrain	0.879	0.879	0.894	0.901	0.813	0.883	0.816	0.891	0.882
NonInvasiveFetalECGThorax1	0.828	0.821	0.861	0.878	0.744	0.844	0.160	0.860	0.832
NonInvasiveFetalECGThorax2	0.870	0.881	0.902	0.910	0.778	0.871	0.227	0.885	0.877
OSULeaf	0.886	0.905	0.904	0.900	0.822	0.898	0.773	0.894	0.900
Plane	0.984	0.973	0.984	0.977	0.953	0.991	0.820	0.968	1.00
PowerCons	0.965	0.863	0.973	0.972	0.959	0.979	0.979	0.979	0.979
RefrigerationDevices	0.576	0.565	0.600	0.605	0.597	0.611	0.589	0.571	0.560
ScreenType	0.472	0.397	0.525	0.491	0.533	0.624	0.528	0.491	0.512
SemgHandGenderCh2	0.845	0.660	0.773	0.862	0.868	0.885	0.878	0.854	0.879
SemgHandMovementCh2	0.884	0.422	0.656	0.867	0.724	0.840	0.511	0.849	0.836
SemgHandSubjectCh2	0.907	0.676	0.829	0.900	0.829	0.898	0.818	0.889	0.913
ShapesAll	0.832	0.742	0.820	0.823	0.620	0.777	0.130	0.800	0.798
SmallKitchenAppliances	0.643	0.613	0.661	0.669	0.731	0.752	0.693	0.661	0.704
StarLightCurves	0.961	0.896	0.946	0.959	0.946	0.956	0.953	0.959	0.961
Strawberry	0.962	0.835	0.918	0.967	0.940	0.936	0.960	0.958	0.952
SwedishLeaf	0.937	0.904	0.930	0.957	0.844	0.927	0.682	0.944	0.923
Trace	0.827	0.942	0.934	0.947	0.867	0.929	0.750	0.915	0.916
TwoPatterns	0.999	0.959	0.999	1.00	0.979	0.995	0.747	0.999	0.999
UWaveGestureLibraryAll	0.962	0.928	0.949	0.972	0.879	0.955	0.894	0.953	0.960
UWaveGestureLibraryX	0.787	0.717	0.775	0.817	0.718	0.800	0.714	0.780	0.789
UWaveGestureLibraryY	0.743	0.644	0.711	0.764	0.646	0.738	0.592	0.729	0.734
UWaveGestureLibraryZ	0.737	0.651	0.729	0.752	0.655	0.740	0.630	0.738	0.730
Wafer	1.00	0.992	1.00	1.00	0.995	1.00	0.995	1.00	1.00
Worms	0.597	0.470	0.644	0.662	0.571	0.599	0.394	0.659	0.602
WormsTwoClass	0.814	0.723	0.765	0.807	0.731	0.811	0.792	0.792	0.811
Yoga	0.896	0.879	0.904	0.904	0.868	0.908	0.893	0.898	0.907

Table 13: Mean and standard deviation of balanced accuracy for TSFresh-20 across 10 random seeds.

	KNN	NB	LR	SVM	DT	RF	AB	MLP	DLN
ACSF1	0.763 ± 0.024	0.720 ± 0.0	0.734 ± 9.7e-03	0.778 ± 0.018	0.630 ± 0.029	0.837 ± 0.019	0.554 ± 0.063	0.763 ± 0.016	0.745 ± 0.038
ChlorineConcentration	0.662 ± 1.1e-03	0.423 ± 0.0	0.468 ± 6.9e-03	0.744 ± 9.7e-03	0.518 ± 0.043	0.536 ± 0.028	0.455 ± 7.4e-03	0.662 ± 0.014	0.570 ± 0.023
Computers	0.641 ± 7.6e-03	0.576 ± 0.0	0.692 ± 3.0e-03	0.663 ± 0.015	0.576 ± 0.026	0.683 ± 0.018	0.696 ± 0.017	0.621 ± 0.020	0.650 ± 0.024
CricketX	0.637 ± 0.020	0.542 ± 0.0	0.583 ± 6.7e-03	0.636 ± 0.022	0.447 ± 0.017	0.601 ± 0.029	0.417 ± 0.025	0.590 ± 0.019	0.574 ± 0.018
CricketY	0.665 ± 3.1e-03	0.531 ± 0.0	0.600 ± 0.025	0.674 ± 0.012	0.495 ± 0.029	0.622 ± 0.029	0.410 ± 0.024	0.621 ± 7.9e-03	0.583 ± 0.031
CricketZ	0.649 ± 6.2e-03	0.567 ± 0.0	0.549 ± 0.035	0.644 ± 0.019	0.472 ± 0.013	0.570 ± 0.010	0.412 ± 0.021	0.571 ± 0.023	0.574 ± 0.019
EOGHorizontalSignal	0.422 ± 0.022	0.478 ± 0.0	0.497 ± 3.1e-03	0.470 ± 0.013	0.488 ± 0.024	0.529 ± 0.014	0.289 ± 0.050	0.477 ± 0.026	0.468 ± 0.025
EOGVerticalSignal	0.425 ± 0.012	0.391 ± 0.0	0.455 ± 4.8e-03	0.440 ± 0.033	0.447 ± 7.9e-03	0.478 ± 0.014	0.406 ± 0.035	0.441 ± 0.026	0.447 ± 0.015
Earthquakes	0.552 ± 0.024	0.650 ± 0.0	0.648 ± 0.018	0.645 ± 0.017	0.597 ± 0.047	0.628 ± 0.015	0.579 ± 0.011	0.573 ± 0.062	0.610 ± 0.034
EthanolLevel	0.354 ± 0.010	0.414 ± 0.0	0.451 ± 0.015	0.411 ± 8.5e-03	0.344 ± 0.016	0.391 ± 0.013	0.349 ± 0.013	0.408 ± 0.023	0.412 ± 0.019
FaceAll	0.811 ± 4.1e-03	0.707 ± 0.0	0.773 ± 8.7e-03	0.826 ± 7.9e-03	0.634 ± 7.6e-03	0.775 ± 0.011	0.525 ± 0.041	0.779 ± 9.0e-03	0.781 ± 8.2e-03
Fish	0.867 ± 0.015	0.855 ± 0.0	0.848 ± 0.019	0.859 ± 0.015	0.688 ± 0.029	0.852 ± 0.015	0.709 ± 0.028	0.841 ± 0.022	0.841 ± 0.018
FordA	1.00 ± 0.0	1.00 ± 0.0	1.00 ± 0.0	1.00 ± 0.0	1.00 ± 0.0	1.00 ± 0.0	1.00 ± 0.0	1.00 ± 0.0	1.00 ± 0.0
FordB	0.781 ± 7.8e-03	0.699 ± 0.0	0.787 ± 8.7e-04	0.807 ± 6.5e-03	0.732 ± 0.014	0.777 ± 0.014	0.764 ± 7.2e-03	0.769 ± 0.014	0.782 ± 0.011
FreezerRegularTrain	0.896 ± 3.0e-03	0.890 ± 0.0	0.931 ± 8.7e-03	0.940 ± 3.1e-03	0.919 ± 0.0	0.949 ± 0.014	0.946 ± 0.012	0.929 ± 6.8e-03	0.939 ± 6.3e-03
GunPointAgeSpan	0.969 ± 8.6e-03	0.915 ± 0.0	0.937 ± 8.1e-03	0.933 ± 9.8e-03	0.939 ± 2.7e-03	0.956 ± 6.4e-03	0.950 ± 2.7e-03	0.965 ± 9.7e-03	0.955 ± 0.012
GunPointMaleVersusFemale	0.983 ± 5.7e-03	0.973 ± 0.0	0.991 ± 1.7e-04	0.992 ± 1.6e-03	0.965 ± 0.0	0.968 ± 3.6e-03	0.972 ± 0.0	0.989 ± 5.4e-03	0.993 ± 7.9e-03
GunPointOldVersusYoung	1.00 ± 0.0	1.00 ± 0.0	1.00 ± 0.0	1.00 ± 0.0	0.999 ± 1.4e-03	1.00 ± 0.0	0.999 ± 1.4e-03	1.00 ± 0.0	1.00 ± 1.1e-03
Ham	0.629 ± 0.035	0.722 ± 0.0	0.607 ± 0.041	0.616 ± 0.021	0.599 ± 0.076	0.669 ± 0.028	0.641 ± 0.021	0.577 ± 0.046	0.640 ± 0.030
HandOutlines	0.851 ± 8.9e-03	0.781 ± 0.0	0.830 ± 1.2e-03	0.858 ± 7.1e-03	0.841 ± 0.015	0.897 ± 6.6e-03	0.837 ± 0.010	0.852 ± 0.017	0.877 ± 9.6e-03
Haptics	0.410 ± 5.1e-03	0.365 ± 0.0	0.434 ± 5.0e-03	0.461 ± 0.023	0.362 ± 0.023	0.449 ± 0.022	0.377 ± 0.012	0.419 ± 0.035	0.437 ± 0.023
InlineSkate	0.375 ± 0.033	0.327 ± 0.0	0.335 ± 5.7e-03	0.346 ± 0.014	0.335 ± 0.014	0.398 ± 0.029	0.261 ± 0.025	0.335 ± 0.027	0.374 ± 0.043
InsectWingbeatSound	0.608 ± 0.012	0.593 ± 0.0	0.556 ± 0.039	0.561 ± 0.021	0.500 ± 8.0e-03	0.625 ± 8.0e-03	0.452 ± 0.045	0.543 ± 0.019	0.572 ± 0.015
LargeKitchenAppliances	0.841 ± 8.2e-03	0.672 ± 0.0	0.803 ± 3.3e-03	0.846 ± 0.010	0.764 ± 0.025	0.878 ± 9.1e-03	0.825 ± 8.7e-03	0.849 ± 0.014	0.851 ± 8.8e-03
MixedShapesRegularTrain	0.914 ± 7.2e-03	0.886 ± 0.0	0.918 ± 7.7e-03	0.939 ± 1.8e-03	0.864 ± 0.012	0.921 ± 3.6e-03	0.867 ± 0.011	0.926 ± 4.4e-03	0.933 ± 5.4e-03

continued on next page

Table 13 (continued)

	KNN	NB	LR	SVM	DT	RF	AB	MLP	DLN
MixedShapesSmallTrain	0.876 $\pm 3.1\text{e-}03$	0.879 ± 0.0	0.876 ± 0.013	0.896 $\pm 2.9\text{e-}03$	0.784 ± 0.020	0.874 $\pm 6.7\text{e-}03$	0.804 $\pm 9.3\text{e-}03$	0.879 $\pm 8.5\text{e-}03$	0.863 ± 0.014
NonInvasiveFetalECGThorax1	0.824 $\pm 3.2\text{e-}03$	0.821 ± 0.0	0.853 $\pm 7.2\text{e-}03$	0.876 $\pm 1.9\text{e-}03$	0.724 ± 0.012	0.833 ± 0.012	0.111 ± 0.025	0.852 $\pm 6.2\text{e-}03$	0.825 $\pm 9.3\text{e-}03$
NonInvasiveFetalECGThorax2	0.867 $\pm 2.1\text{e-}03$	0.881 ± 0.0	0.890 $\pm 9.8\text{e-}03$	0.906 $\pm 1.9\text{e-}03$	0.764 ± 0.013	0.841 ± 0.031	0.202 ± 0.023	0.876 $\pm 6.9\text{e-}03$	0.861 ± 0.017
OSULeaf	0.863 ± 0.013	0.905 ± 0.0	0.888 ± 0.023	0.896 $\pm 3.7\text{e-}03$	0.801 ± 0.022	0.887 ± 0.010	0.763 $\pm 9.7\text{e-}03$	0.866 ± 0.018	0.864 ± 0.020
Plane	0.946 ± 0.024	0.973 ± 0.0	0.970 ± 0.013	0.973 $\pm 4.3\text{e-}03$	0.898 ± 0.023	0.980 ± 0.016	0.713 ± 0.15	0.951 ± 0.013	0.974 ± 0.013
PowerCons	0.952 $\pm 9.9\text{e-}03$	0.863 ± 0.0	0.963 $\pm 8.7\text{e-}03$	0.966 $\pm 7.9\text{e-}03$	0.943 ± 0.020	0.959 ± 0.025	0.974 $\pm 4.7\text{e-}03$	0.968 $\pm 8.0\text{e-}03$	0.968 $\pm 9.3\text{e-}03$
RefrigerationDevices	0.552 ± 0.014	0.565 ± 0.0	0.587 ± 0.013	0.577 ± 0.029	0.555 ± 0.021	0.593 ± 0.011	0.550 ± 0.025	0.534 ± 0.025	0.541 ± 0.018
ScreenType	0.458 ± 0.010	0.397 ± 0.0	0.498 ± 0.011	0.473 ± 0.017	0.502 ± 0.037	0.570 ± 0.027	0.507 $\pm 8.7\text{e-}03$	0.475 ± 0.012	0.485 ± 0.020
SemgHandGenderCh2	0.826 $\pm 9.2\text{e-}03$	0.660 ± 0.0	0.769 $\pm 2.9\text{e-}03$	0.847 $\pm 8.8\text{e-}03$	0.853 ± 0.015	0.870 ± 0.012	0.868 $\pm 8.3\text{e-}03$	0.835 ± 0.012	0.869 ± 0.010
SemgHandMovementCh2	0.860 ± 0.016	0.422 ± 0.0	0.645 $\pm 3.7\text{e-}03$	0.843 ± 0.020	0.716 $\pm 7.3\text{e-}03$	0.822 ± 0.017	0.467 ± 0.029	0.830 ± 0.011	0.798 ± 0.027
SemgHandSubjectCh2	0.895 $\pm 9.5\text{e-}03$	0.676 ± 0.0	0.820 $\pm 9.9\text{e-}03$	0.888 ± 0.015	0.807 ± 0.016	0.887 ± 0.011	0.797 ± 0.012	0.866 ± 0.020	0.901 $\pm 6.9\text{e-}03$
ShapesAll	0.832 ± 0.0	0.741 $\pm 8.1\text{e-}04$	0.802 ± 0.016	0.815 $\pm 3.8\text{e-}03$	0.608 $\pm 6.7\text{e-}03$	0.712 ± 0.054	0.103 ± 0.013	0.782 ± 0.013	0.784 $\pm 7.2\text{e-}03$
SmallKitchenAppliances	0.634 ± 0.014	0.613 ± 0.0	0.644 $\pm 6.3\text{e-}03$	0.661 $\pm 7.3\text{e-}03$	0.703 ± 0.023	0.741 $\pm 6.1\text{e-}03$	0.673 ± 0.015	0.628 ± 0.024	0.668 ± 0.019
StarLightCurves	0.960 $\pm 5.9\text{e-}04$	0.896 ± 0.0	0.944 $\pm 2.1\text{e-}03$	0.958 $\pm 1.1\text{e-}03$	0.944 $\pm 2.0\text{e-}03$	0.954 $\pm 1.8\text{e-}03$	0.950 $\pm 2.9\text{e-}03$	0.955 $\pm 3.4\text{e-}03$	0.955 $\pm 3.2\text{e-}03$
Strawberry	0.957 $\pm 5.1\text{e-}03$	0.835 ± 0.0	0.914 $\pm 2.0\text{e-}03$	0.957 $\pm 7.1\text{e-}03$	0.925 $\pm 7.7\text{e-}03$	0.928 $\pm 5.6\text{e-}03$	0.951 $\pm 4.9\text{e-}03$	0.945 ± 0.010	0.942 $\pm 5.6\text{e-}03$
SwedishLeaf	0.927 $\pm 6.3\text{e-}03$	0.904 ± 0.0	0.925 $\pm 3.2\text{e-}03$	0.942 $\pm 7.5\text{e-}03$	0.826 ± 0.014	0.915 $\pm 9.8\text{e-}03$	0.604 ± 0.066	0.924 ± 0.010	0.912 ± 0.013
Trace	0.820 ± 0.017	0.942 ± 0.0	0.900 ± 0.030	0.935 $\pm 8.6\text{e-}03$	0.851 ± 0.013	0.884 ± 0.029	0.716 ± 0.013	0.874 ± 0.022	0.899 ± 0.021
TwoPatterns	0.998 $\pm 1.8\text{e-}03$	0.959 ± 0.0	0.995 $\pm 4.9\text{e-}03$	0.999 $\pm 3.2\text{e-}04$	0.978 $\pm 1.2\text{e-}03$	0.993 $\pm 2.8\text{e-}03$	0.746 $\pm 9.3\text{e-}04$	0.997 $\pm 2.3\text{e-}03$	0.997 $\pm 1.6\text{e-}03$
UWaveGestureLibraryAll	0.959 $\pm 2.2\text{e-}03$	0.928 ± 0.0	0.944 $\pm 5.3\text{e-}03$	0.968 $\pm 5.0\text{e-}03$	0.874 $\pm 3.9\text{e-}03$	0.947 $\pm 4.5\text{e-}03$	0.879 $\pm 8.5\text{e-}03$	0.947 $\pm 5.3\text{e-}03$	0.953 $\pm 4.5\text{e-}03$
UWaveGestureLibraryX	0.786 $\pm 7.4\text{e-}04$	0.717 ± 0.0	0.766 $\pm 4.9\text{e-}03$	0.808 $\pm 7.9\text{e-}03$	0.706 $\pm 6.2\text{e-}03$	0.785 ± 0.016	0.707 $\pm 6.8\text{e-}03$	0.763 $\pm 8.3\text{e-}03$	0.778 $\pm 8.6\text{e-}03$
UWaveGestureLibraryY	0.742 $\pm 2.1\text{e-}03$	0.644 ± 0.0	0.706 $\pm 2.8\text{e-}03$	0.755 ± 0.011	0.639 $\pm 5.9\text{e-}03$	0.728 $\pm 7.8\text{e-}03$	0.567 ± 0.014	0.713 $\pm 7.5\text{e-}03$	0.720 $\pm 7.6\text{e-}03$
UWaveGestureLibraryZ	0.730 $\pm 5.2\text{e-}03$	0.651 ± 0.0	0.722 $\pm 7.2\text{e-}03$	0.745 $\pm 4.6\text{e-}03$	0.637 ± 0.011	0.724 ± 0.016	0.613 ± 0.014	0.723 $\pm 9.2\text{e-}03$	0.721 $\pm 5.3\text{e-}03$
Wafer	1.00 ± 0.0	0.992 ± 0.0	1.00 ± 0.0	1.00 ± 0.0	0.994 $\pm 1.6\text{e-}03$	0.999 $\pm 7.8\text{e-}04$	0.994 $\pm 1.6\text{e-}03$	1.00 $\pm 5.1\text{e-}04$	0.998 $\pm 2.9\text{e-}03$
Worms	0.561 ± 0.072	0.470 ± 0.0	0.612 ± 0.046	0.622 ± 0.022	0.515 ± 0.031	0.536 ± 0.029	0.360 ± 0.029	0.560 ± 0.064	0.525 ± 0.055
WormsTwoClass	0.769 ± 0.028	0.723 ± 0.0	0.755 $\pm 7.8\text{e-}03$	0.780 ± 0.028	0.706 ± 0.029	0.767 ± 0.031	0.777 ± 0.013	0.742 ± 0.035	0.792 ± 0.013
Yoga	0.895 $\pm 1.2\text{e-}03$	0.879 ± 0.0	0.897 $\pm 4.2\text{e-}03$	0.899 $\pm 3.5\text{e-}03$	0.856 $\pm 8.9\text{e-}03$	0.902 $\pm 3.5\text{e-}03$	0.888 $\pm 3.7\text{e-}03$	0.888 $\pm 9.1\text{e-}03$	0.891 $\pm 9.6\text{e-}03$

Table 14: Geometric mean of inference OPs for TSFresh-20 across 10 random seeds assuming FP16 for floating-point and INT16 for integer arithmetic.

	KNN	NB	LR	SVM	DT	RF	AB	MLP	DLN
ACSF1	829K	2.19M	1.70M	7.10M	897	161K	227K	3.68M	43.1K
ChlorineConcentration	11.4M	656K	511K	17.6M	1.83K	116K	244K	6.03M	50.2K
Computers	1.57M	438K	170K	11.7M	897	121K	195K	2.91M	28.1K
CricketX	2.50M	2.63M	2.04M	37.7M	1.50K	171K	248K	4.79M	64.7K
CricketY	4.25M	2.63M	2.04M	60.9M	1.45K	182K	258K	4.30M	63.5K
CricketZ	2.50M	2.63M	2.04M	64.4M	1.56K	152K	274K	4.71M	68.9K
Earthquakes	6.43M	423K	168K	10.3M	897	15.7K	217K	1.64M	24.2K
EOGHorizontalSignal	2.31M	2.63M	2.04M	37.7M	1.24K	176K	214K	4.47M	65.3K
EOGVerticalSignal	2.31M	2.63M	2.04M	35.0M	1.45K	190K	257K	3.18M	52.8K
EthanolLevel	4.39M	875K	681K	24.3M	750	160K	163K	2.66M	33.9K
FaceAll	3.64M	3.06M	2.38M	68.0M	1.54K	198K	263K	6.23M	66.9K
Fish	1.08M	1.53M	1.19M	10.5M	1.12K	152K	229K	4.10M	38.0K
FordA	33.3M	438K	170K	28.1M	183	19.3K	136K	3.98M	2.24K
FordB	40.0M	430K	169K	40.6M	1.32K	181K	260K	2.35M	41.1K
FreezerRegularTrain	2.94M	438K	170K	2.02M	183	49.7K	159K	3.35M	8.21K
GunPointAgeSpan	1.18M	445K	171K	1.54M	549	84.3K	194K	2.41M	22.8K
GunPointMaleVersusFemale	1.81M	445K	171K	1.92M	183	32.6K	146K	4.30M	9.99K
GunPointOldVersusYoung	1.24M	452K	173K	3.37M	183	24.1K	136K	4.78M	6.71K
Ham	906K	438K	170K	2.73M	512	88.6K	161K	3.16M	29.7K
HandOutlines	8.90M	438K	170K	59.9M	1.23K	160K	263K	2.52M	30.2K
Haptics	2.34M	1.09M	851K	17.1M	952	126K	225K	3.30M	34.1K
InlineSkate	821K	1.53M	1.19M	3.18M	1.01K	119K	226K	4.68M	39.7K
InsectWingbeatSound	1.38M	2.41M	1.87M	25.8M	1.15K	153K	256K	4.49M	52.7K
LargeKitchenAppliances	2.40M	656K	511K	15.8M	1.13K	177K	241K	5.25M	39.3K
MixedShapesRegularTrain	8.84M	1.09M	851K	32.1M	1.32K	185K	222K	5.82M	40.6K
MixedShapesSmallTrain	2.85M	1.09M	851K	3.97M	677	102K	188K	3.45M	39.8K
NonInvasiveFetalECGThorax1	12.3M	9.19M	7.15M	250M	1.88K	191K	246K	5.46M	175K
NonInvasiveFetalECGThorax2	12.3M	9.19M	7.15M	139M	1.90K	148K	251K	5.26M	162K
OSULeaf	2.59M	1.31M	1.02M	13.3M	695	121K	185K	3.39M	45.5K
Plane	637K	1.53M	1.19M	5.05M	1.04K	85.0K	222K	3.12M	28.4K
PowerCons	1.95M	445K	171K	2.43M	586	62.5K	183K	4.00M	15.0K
RefrigerationDevices	2.40M	656K	511K	27.6M	1.30K	176K	227K	3.69M	33.4K
ScreenType	2.40M	656K	511K	18.9M	878	162K	218K	2.67M	39.2K
SemgHandGenderCh2	1.90M	438K	170K	13.1M	952	143K	210K	2.43M	53.6K
SemgHandMovementCh2	2.90M	1.31M	1.02M	41.9M	1.41K	153K	236K	7.55M	54.2K
SemgHandSubjectCh2	2.90M	1.09M	851K	45.2M	1.59K	206K	224K	4.62M	73.1K
ShapesAll	4.06M	13.4M	10.3M	87.8M	1.72K	160K	245K	7.68M	204K
SmallKitchenAppliances	3.24M	656K	511K	24.7M	915	180K	175K	2.98M	30.9K
StarLightCurves	6.66M	656K	511K	27.4M	403	120K	149K	4.72M	24.0K
Strawberry	10.9M	438K	170K	14.9M	1.10K	120K	235K	4.41M	24.6K
SwedishLeaf	4.36M	3.28M	2.55M	43.2M	1.21K	168K	255K	7.92M	76.7K
Trace	721K	830K	666K	1.94M	586	95.5K	193K	2.33M	17.1K
TwoPatterns	8.90M	875K	681K	8.38M	1.19K	167K	197K	4.50M	28.4K
UWaveGestureLibraryAll	5.94M	1.75M	1.36M	64.1M	1.23K	197K	258K	6.05M	56.7K
UWaveGestureLibraryX	5.94M	1.75M	1.36M	85.7M	1.61K	164K	242K	3.15M	54.3K
UWaveGestureLibraryY	5.94M	1.75M	1.36M	110M	1.85K	149K	197K	5.12M	66.0K
UWaveGestureLibraryZ	9.96M	1.75M	1.36M	92.0M	1.56K	171K	236K	4.40M	82.0K
Wafer	8.90M	438K	170K	9.72M	183	23.7K	136K	3.98M	4.59K
Worms	4.16M	1.09M	851K	15.2M	512	70.3K	211K	2.53M	25.7K
WormsTwoClass	1.27M	430K	169K	17.2M	787	56.2K	191K	2.49M	29.8K
Yoga	1.98M	445K	171K	6.16M	897	156K	195K	3.83M	17.2K

Table 15: Best-of-10 test balanced accuracy for TSFresh-40.

	KNN	NB	LR	SVM	DT	RF	AB	MLP	DLN
ACSF1	0.750	0.740	0.730	0.770	0.710	0.880	0.630	0.770	0.810
ChlorineConcentration	0.682	0.408	0.574	0.784	0.560	0.583	0.500	0.736	0.665
Computers	0.688	0.584	0.680	0.700	0.660	0.696	0.688	0.676	0.716
CricketX	0.642	0.555	0.624	0.657	0.478	0.624	0.458	0.632	0.631
CricketY	0.721	0.544	0.657	0.765	0.532	0.664	0.484	0.697	0.679
CricketZ	0.683	0.615	0.619	0.643	0.501	0.615	0.443	0.628	0.642
Earthquakes	0.566	0.659	0.689	0.707	0.702	0.689	0.557	0.600	0.718
EOGHorizontalSignal	0.456	0.492	0.537	0.537	0.551	0.562	0.338	0.554	0.573
EOGVerticalSignal	0.471	0.375	0.460	0.468	0.476	0.496	0.475	0.469	0.480
EthanolLevel	0.340	0.431	0.466	0.438	0.364	0.390	0.361	0.464	0.421
FaceAll	0.832	0.824	0.834	0.856	0.674	0.819	0.642	0.841	0.838
Fish	0.866	0.792	0.872	0.867	0.709	0.903	0.735	0.886	0.891
FordA	1.00	0.999	1.00	1.00	1.00	1.00	1.00	1.00	1.00
FordB	0.808	0.621	0.802	0.837	0.760	0.817	0.783	0.830	0.817
FreezerRegularTrain	0.870	0.861	0.946	0.953	0.945	0.976	0.974	0.945	0.951
GunPointAgeSpan	0.990	0.914	0.962	0.962	0.940	0.969	0.972	0.978	0.974
GunPointMaleVersusFemale	0.993	0.967	0.994	0.997	0.965	0.975	0.972	0.997	1.00
GunPointOldVersusYoung	1.00	1.00	1.00	1.00	1.00	1.00	1.00	1.00	1.00
Ham	0.654	0.733	0.771	0.655	0.697	0.742	0.715	0.643	0.711
HandOutlines	0.851	0.725	0.870	0.895	0.879	0.896	0.859	0.904	0.899
Haptics	0.438	0.361	0.474	0.495	0.434	0.508	0.459	0.487	0.492
InlineSkate	0.446	0.328	0.369	0.404	0.395	0.477	0.348	0.414	0.462
InsectWingbeatSound	0.636	0.604	0.630	0.636	0.497	0.656	0.472	0.599	0.637
LargeKitchenAppliances	0.821	0.683	0.816	0.861	0.861	0.891	0.872	0.835	0.869
MixedShapesRegularTrain	0.932	0.888	0.932	0.944	0.871	0.928	0.897	0.931	0.941
MixedShapesSmallTrain	0.872	0.877	0.889	0.901	0.813	0.890	0.823	0.897	0.888
NonInvasiveFetalECGThorax1	0.860	0.860	0.891	0.901	0.765	0.873	0.216	0.893	0.883
NonInvasiveFetalECGThorax2	0.891	0.895	0.915	0.924	0.798	0.894	0.296	0.904	0.915
OSULeaf	0.852	0.852	0.892	0.903	0.828	0.898	0.773	0.875	0.877
Plane	1.00	1.00	1.00	1.00	0.988	1.00	0.865	1.00	1.00
PowerCons	0.959	0.876	0.979	0.979	0.938	0.972	0.993	0.993	0.986
RefrigerationDevices	0.531	0.541	0.560	0.565	0.573	0.608	0.565	0.568	0.573
ScreenType	0.459	0.424	0.541	0.557	0.597	0.589	0.541	0.531	0.573
SemgHandGenderCh2	0.864	0.664	0.873	0.891	0.871	0.925	0.932	0.884	0.912
SemgHandMovementCh2	0.824	0.420	0.662	0.789	0.736	0.858	0.531	0.800	0.824
SemgHandSubjectCh2	0.896	0.662	0.820	0.882	0.844	0.904	0.831	0.873	0.916
ShapesAll	0.762	0.752	0.760	0.765	0.602	0.788	0.148	0.762	0.808
SmallKitchenAppliances	0.725	0.731	0.784	0.773	0.731	0.795	0.792	0.765	0.813
StarLightCurves	0.961	0.928	0.955	0.962	0.945	0.958	0.958	0.960	0.961
Strawberry	0.968	0.841	0.937	0.971	0.950	0.953	0.980	0.966	0.964
SwedishLeaf	0.936	0.896	0.955	0.958	0.849	0.938	0.675	0.953	0.943
Trace	1.00	0.991	1.00	1.00	1.00	1.00	1.00	1.00	1.00
TwoPatterns	0.998	0.961	0.998	0.999	0.986	0.997	0.748	0.999	0.999
UWaveGestureLibraryAll	0.960	0.915	0.960	0.973	0.874	0.951	0.899	0.958	0.964
UWaveGestureLibraryX	0.779	0.711	0.779	0.811	0.743	0.806	0.728	0.783	0.802
UWaveGestureLibraryY	0.747	0.645	0.721	0.768	0.662	0.733	0.596	0.736	0.743
UWaveGestureLibraryZ	0.748	0.662	0.748	0.765	0.696	0.753	0.678	0.761	0.754
Wafer	1.00	0.992	1.00	1.00	0.995	1.00	0.995	1.00	1.00
Worms	0.631	0.522	0.667	0.679	0.604	0.673	0.637	0.698	0.693
WormsTwoClass	0.826	0.750	0.803	0.818	0.777	0.833	0.803	0.814	0.822
Yoga	0.908	0.894	0.897	0.906	0.876	0.897	0.903	0.907	0.913

Table 16: Mean and standard deviation of balanced accuracy for TSFresh-40 across 10 random seeds.

	KNN	NB	LR	SVM	DT	RF	AB	MLP	DLN
ACSF1	0.733 ± 0.023	0.737 $\pm 6.7\text{e-}03$	0.685 ± 0.037	0.742 ± 0.021	0.660 ± 0.033	0.848 ± 0.019	0.521 ± 0.048	0.726 ± 0.033	0.761 ± 0.020
ChlorineConcentration	0.682 $\pm 3.3\text{e-}05$	0.408 ± 0.0	0.566 ± 0.010	0.776 ± 0.010	0.525 ± 0.031	0.556 ± 0.026	0.474 ± 0.015	0.705 ± 0.018	0.646 ± 0.014
Computers	0.672 ± 0.013	0.584 ± 0.0	0.667 $\pm 7.8\text{e-}03$	0.674 ± 0.013	0.620 ± 0.032	0.679 $\pm 9.8\text{e-}03$	0.672 ± 0.012	0.656 ± 0.014	0.659 ± 0.035
CricketX	0.636 $\pm 5.3\text{e-}03$	0.555 ± 0.0	0.607 ± 0.017	0.644 $\pm 9.1\text{e-}03$	0.452 ± 0.015	0.597 ± 0.017	0.408 ± 0.028	0.603 ± 0.014	0.602 ± 0.022
CricketY	0.705 ± 0.013	0.544 ± 0.0	0.641 ± 0.018	0.740 ± 0.025	0.504 ± 0.016	0.646 ± 0.012	0.446 ± 0.019	0.678 ± 0.018	0.644 ± 0.024
CricketZ	0.666 ± 0.010	0.615 ± 0.0	0.589 ± 0.028	0.613 ± 0.022	0.471 ± 0.029	0.596 ± 0.022	0.404 ± 0.020	0.590 ± 0.026	0.611 ± 0.020
EOGHorizontalSignal	0.434 $\pm 7.9\text{e-}03$	0.492 ± 0.0	0.514 ± 0.018	0.520 ± 0.012	0.520 ± 0.019	0.545 ± 0.013	0.295 ± 0.044	0.505 ± 0.045	0.503 ± 0.036
EOGVerticalSignal	0.466 $\pm 4.1\text{e-}03$	0.375 ± 0.0	0.442 ± 0.011	0.448 ± 0.017	0.425 ± 0.027	0.489 $\pm 6.6\text{e-}03$	0.414 ± 0.029	0.450 ± 0.018	0.454 ± 0.022
Earthquakes	0.539 $\pm 9.6\text{e-}03$	0.659 ± 0.0	0.667 ± 0.013	0.675 ± 0.017	0.632 ± 0.055	0.655 ± 0.016	0.540 ± 0.016	0.565 ± 0.025	0.643 ± 0.043
EthanolLevel	0.330 $\pm 4.8\text{e-}03$	0.431 ± 0.0	0.454 ± 0.012	0.410 ± 0.018	0.348 ± 0.014	0.377 $\pm 8.0\text{e-}03$	0.340 ± 0.012	0.431 ± 0.021	0.403 ± 0.016
FaceAll	0.831 $\pm 4.5\text{e-}03$	0.824 ± 0.0	0.816 ± 0.014	0.850 $\pm 4.7\text{e-}03$	0.665 $\pm 6.9\text{e-}03$	0.808 $\pm 6.1\text{e-}03$	0.576 ± 0.037	0.829 $\pm 8.9\text{e-}03$	0.827 ± 0.013
Fish	0.851 ± 0.014	0.788 $\pm 3.1\text{e-}03$	0.859 $\pm 5.9\text{e-}03$	0.854 $\pm 7.5\text{e-}03$	0.678 ± 0.019	0.864 ± 0.022	0.676 ± 0.029	0.865 ± 0.017	0.870 ± 0.017
FordA	1.00 ± 0.0	0.999 ± 0.0	1.00 ± 0.0	1.00 ± 0.0	1.00 ± 0.0	1.00 ± 0.0	1.00 ± 0.0	1.00 ± 0.0	1.00 ± 0.0
FordB	0.800 $\pm 3.6\text{e-}03$	0.621 ± 0.0	0.800 $\pm 8.3\text{e-}04$	0.831 $\pm 5.8\text{e-}03$	0.739 ± 0.018	0.803 $\pm 7.9\text{e-}03$	0.771 $\pm 9.1\text{e-}03$	0.807 ± 0.011	0.805 ± 0.010
FreezerRegularTrain	0.859 $\pm 7.0\text{e-}03$	0.861 ± 0.0	0.942 $\pm 3.6\text{e-}03$	0.944 $\pm 4.6\text{e-}03$	0.924 ± 0.011	0.952 ± 0.017	0.963 ± 0.014	0.937 $\pm 7.2\text{e-}03$	0.945 $\pm 3.6\text{e-}03$
GunPointAgeSpan	0.983 $\pm 3.2\text{e-}03$	0.914 ± 0.0	0.938 ± 0.017	0.935 ± 0.012	0.940 ± 0.0	0.963 $\pm 3.7\text{e-}03$	0.964 $\pm 9.6\text{e-}03$	0.968 ± 0.011	0.962 ± 0.011
GunPointMaleVersusFemale	0.987 $\pm 6.6\text{e-}03$	0.967 ± 0.0	0.993 $\pm 1.6\text{e-}03$	0.990 $\pm 9.3\text{e-}03$	0.965 ± 0.0	0.969 $\pm 4.3\text{e-}03$	0.972 ± 0.0	0.992 $\pm 4.1\text{e-}03$	0.993 $\pm 5.8\text{e-}03$
GunPointOldVersusYoung	1.00 ± 0.0	1.00 ± 0.0	1.00 ± 0.0	1.00 ± 0.0	1.00 $\pm 1.1\text{e-}03$	1.00 ± 0.0	0.999 $\pm 1.6\text{e-}03$	1.00 ± 0.0	1.00 ± 0.0
Ham	0.617 ± 0.031	0.733 ± 0.0	0.653 ± 0.060	0.611 ± 0.022	0.623 ± 0.052	0.691 ± 0.029	0.674 ± 0.026	0.599 ± 0.033	0.663 ± 0.023
HandOutlines	0.851 $\pm 5.7\text{e-}04$	0.725 ± 0.0	0.865 $\pm 3.5\text{e-}03$	0.886 ± 0.012	0.869 $\pm 8.7\text{e-}03$	0.893 $\pm 1.9\text{e-}03$	0.845 $\pm 8.4\text{e-}03$	0.885 ± 0.016	0.880 ± 0.011
Haptics	0.398 ± 0.027	0.361 ± 0.0	0.434 ± 0.037	0.462 ± 0.038	0.394 ± 0.036	0.469 ± 0.019	0.430 ± 0.017	0.439 ± 0.023	0.467 ± 0.016
InlineSkate	0.426 ± 0.028	0.328 ± 0.0	0.338 ± 0.025	0.384 ± 0.011	0.368 ± 0.026	0.440 ± 0.039	0.313 ± 0.026	0.366 ± 0.023	0.409 ± 0.029
InsectWingbeatSound	0.630 $\pm 4.2\text{e-}03$	0.604 ± 0.0	0.589 ± 0.042	0.601 ± 0.023	0.478 ± 0.017	0.644 $\pm 9.9\text{e-}03$	0.413 ± 0.045	0.574 ± 0.017	0.609 ± 0.016
LargeKitchenAppliances	0.816 $\pm 9.0\text{e-}03$	0.683 ± 0.0	0.799 ± 0.010	0.848 ± 0.010	0.791 ± 0.045	0.877 $\pm 8.3\text{e-}03$	0.850 ± 0.011	0.821 $\pm 7.8\text{e-}03$	0.853 ± 0.018
MixedShapesRegularTrain	0.926 $\pm 7.8\text{e-}03$	0.888 ± 0.0	0.927 $\pm 6.2\text{e-}03$	0.936 $\pm 5.7\text{e-}03$	0.854 ± 0.013	0.922 $\pm 4.5\text{e-}03$	0.884 $\pm 7.2\text{e-}03$	0.928 $\pm 2.9\text{e-}03$	0.931 $\pm 8.1\text{e-}03$

continued on next page

Table 16 (continued)

	KNN	NB	LR	SVM	DT	RF	AB	MLP	DLN
MixedShapesSmallTrain	0.865 $\pm 4.1\text{e-}03$	0.877 ± 0.0	0.884 $\pm 4.4\text{e-}03$	0.895 $\pm 3.2\text{e-}03$	0.774 ± 0.024	0.880 $\pm 8.1\text{e-}03$	0.797 ± 0.021	0.882 ± 0.014	0.875 ± 0.010
NonInvasiveFetalECGThorax1	0.858 $\pm 2.6\text{e-}03$	0.860 ± 0.0	0.876 ± 0.014	0.897 $\pm 2.7\text{e-}03$	0.744 ± 0.016	0.852 ± 0.017	0.183 ± 0.029	0.883 $\pm 7.2\text{e-}03$	0.869 $\pm 8.3\text{e-}03$
NonInvasiveFetalECGThorax2	0.889 $\pm 2.9\text{e-}03$	0.895 ± 0.0	0.903 $\pm 6.4\text{e-}03$	0.918 $\pm 2.5\text{e-}03$	0.786 $\pm 9.0\text{e-}03$	0.863 ± 0.029	0.246 ± 0.043	0.900 $\pm 2.8\text{e-}03$	0.898 $\pm 9.6\text{e-}03$
OSULeaf	0.829 ± 0.017	0.852 ± 0.0	0.883 $\pm 7.1\text{e-}03$	0.882 ± 0.010	0.807 ± 0.013	0.882 $\pm 8.5\text{e-}03$	0.758 ± 0.013	0.843 ± 0.022	0.861 ± 0.015
Plane	0.981 ± 0.014	1.00 ± 0.0	0.986 $\pm 8.2\text{e-}03$	0.994 $\pm 7.4\text{e-}03$	0.963 ± 0.016	0.991 ± 0.013	0.837 ± 0.051	0.989 ± 0.013	0.988 ± 0.014
PowerCons	0.953 ± 0.013	0.876 ± 0.0	0.972 ± 0.011	0.959 ± 0.013	0.898 ± 0.028	0.944 ± 0.030	0.977 ± 0.012	0.968 ± 0.017	0.973 ± 0.016
RefrigerationDevices	0.515 ± 0.014	0.541 ± 0.0	0.533 ± 0.013	0.549 ± 0.016	0.547 ± 0.022	0.586 ± 0.012	0.530 ± 0.015	0.527 ± 0.023	0.537 ± 0.019
ScreenType	0.448 $\pm 9.8\text{e-}03$	0.424 ± 0.0	0.528 $\pm 6.9\text{e-}03$	0.524 ± 0.025	0.504 ± 0.049	0.559 ± 0.018	0.524 ± 0.016	0.489 ± 0.026	0.521 ± 0.025
SemgHandGenderCh2	0.852 ± 0.013	0.664 ± 0.0	0.852 ± 0.033	0.877 $\pm 8.0\text{e-}03$	0.856 ± 0.016	0.914 ± 0.011	0.919 $\pm 6.2\text{e-}03$	0.865 ± 0.014	0.905 $\pm 7.8\text{e-}03$
SemgHandMovementCh2	0.820 $\pm 5.5\text{e-}03$	0.420 ± 0.0	0.648 $\pm 7.9\text{e-}03$	0.759 ± 0.031	0.705 ± 0.030	0.832 ± 0.018	0.502 ± 0.018	0.770 ± 0.022	0.790 ± 0.031
SemgHandSubjectCh2	0.889 $\pm 6.1\text{e-}03$	0.662 ± 0.0	0.805 ± 0.010	0.868 $\pm 9.9\text{e-}03$	0.820 ± 0.021	0.893 ± 0.014	0.803 ± 0.013	0.859 $\pm 8.8\text{e-}03$	0.901 ± 0.011
ShapesAll	0.762 ± 0.0	0.750 $\pm 2.8\text{e-}03$	0.738 ± 0.020	0.756 $\pm 4.7\text{e-}03$	0.575 ± 0.012	0.745 ± 0.028	0.107 ± 0.018	0.743 ± 0.010	0.783 ± 0.020
SmallKitchenAppliances	0.709 ± 0.016	0.731 ± 0.0	0.773 $\pm 5.5\text{e-}03$	0.763 ± 0.015	0.711 ± 0.019	0.785 $\pm 8.9\text{e-}03$	0.783 $\pm 5.5\text{e-}03$	0.743 ± 0.015	0.774 ± 0.021
StarLightCurves	0.960 $\pm 2.7\text{e-}04$	0.928 ± 0.0	0.953 $\pm 1.6\text{e-}03$	0.960 $\pm 1.7\text{e-}03$	0.944 $\pm 6.1\text{e-}04$	0.956 $\pm 1.6\text{e-}03$	0.953 $\pm 2.5\text{e-}03$	0.958 $\pm 1.5\text{e-}03$	0.957 $\pm 2.8\text{e-}03$
Strawberry	0.960 $\pm 6.1\text{e-}03$	0.841 ± 0.0	0.928 $\pm 5.2\text{e-}03$	0.955 ± 0.013	0.931 ± 0.014	0.941 $\pm 5.7\text{e-}03$	0.966 ± 0.010	0.955 $\pm 6.9\text{e-}03$	0.952 $\pm 9.8\text{e-}03$
SwedishLeaf	0.933 $\pm 2.6\text{e-}03$	0.893 $\pm 4.4\text{e-}03$	0.946 $\pm 6.7\text{e-}03$	0.954 $\pm 2.3\text{e-}03$	0.839 $\pm 7.1\text{e-}03$	0.930 $\pm 4.8\text{e-}03$	0.603 ± 0.038	0.936 $\pm 9.6\text{e-}03$	0.933 $\pm 5.5\text{e-}03$
Trace	0.997 $\pm 6.0\text{e-}03$	0.991 ± 0.0	1.00 ± 0.0	1.00 ± 0.0	0.981 ± 0.018	1.00 ± 0.0	0.852 ± 0.13	1.00 ± 0.0	0.995 ± 0.012
TwoPatterns	0.998 $\pm 2.1\text{e-}04$	0.961 ± 0.0	0.993 $\pm 6.3\text{e-}03$	0.999 $\pm 1.8\text{e-}04$	0.980 $\pm 4.0\text{e-}03$	0.996 $\pm 2.3\text{e-}03$	0.746 $\pm 1.1\text{e-}03$	0.997 $\pm 1.5\text{e-}03$	0.996 $\pm 1.5\text{e-}03$
UWaveGestureLibraryAll	0.952 $\pm 3.7\text{e-}03$	0.915 ± 0.0	0.951 ± 0.012	0.970 $\pm 4.2\text{e-}03$	0.865 $\pm 6.6\text{e-}03$	0.946 $\pm 5.1\text{e-}03$	0.886 $\pm 9.0\text{e-}03$	0.955 $\pm 2.1\text{e-}03$	0.958 $\pm 3.9\text{e-}03$
UWaveGestureLibraryX	0.773 $\pm 3.4\text{e-}03$	0.711 ± 0.0	0.770 $\pm 6.5\text{e-}03$	0.798 ± 0.012	0.715 ± 0.016	0.798 $\pm 7.9\text{e-}03$	0.718 $\pm 7.5\text{e-}03$	0.773 $\pm 7.4\text{e-}03$	0.787 ± 0.010
UWaveGestureLibraryY	0.738 $\pm 8.5\text{e-}03$	0.645 ± 0.0	0.712 $\pm 7.1\text{e-}03$	0.760 $\pm 6.9\text{e-}03$	0.654 $\pm 7.1\text{e-}03$	0.727 $\pm 4.5\text{e-}03$	0.582 ± 0.012	0.724 ± 0.010	0.728 ± 0.012
UWaveGestureLibraryZ	0.738 $\pm 7.5\text{e-}03$	0.662 ± 0.0	0.739 $\pm 7.6\text{e-}03$	0.758 $\pm 6.3\text{e-}03$	0.675 ± 0.017	0.739 ± 0.026	0.646 ± 0.016	0.749 ± 0.012	0.741 ± 0.010
Wafer	1.00 ± 0.0	0.992 ± 0.0	1.00 ± 0.0	1.00 ± 0.0	0.995 $\pm 1.3\text{e-}03$	0.999 $\pm 1.0\text{e-}03$	0.995 $\pm 1.5\text{e-}03$	1.00 $\pm 5.8\text{e-}05$	0.999 $\pm 1.6\text{e-}03$
Worms	0.592 ± 0.024	0.519 $\pm 6.5\text{e-}03$	0.618 ± 0.055	0.663 ± 0.017	0.551 ± 0.025	0.626 ± 0.036	0.546 ± 0.053	0.622 ± 0.053	0.621 ± 0.049
WormsTwoClass	0.787 ± 0.023	0.750 ± 0.0	0.758 ± 0.024	0.792 ± 0.021	0.733 ± 0.033	0.806 ± 0.018	0.780 ± 0.014	0.763 ± 0.033	0.775 ± 0.037
Yoga	0.899 $\pm 6.5\text{e-}03$	0.894 ± 0.0	0.893 $\pm 3.1\text{e-}03$	0.901 $\pm 3.3\text{e-}03$	0.852 ± 0.011	0.892 $\pm 3.9\text{e-}03$	0.897 $\pm 3.1\text{e-}03$	0.897 $\pm 8.2\text{e-}03$	0.894 $\pm 8.2\text{e-}03$

Table 17: Geometric mean of inference OPs for TSFresh-40 across 10 random seeds assuming FP16 for floating-point and INT16 for integer arithmetic.

	KNN	NB	LR	SVM	DT	RF	AB	MLP	DLN
ACSF1	1.10M	2.93M	1.95M	11.2M	1.10K	149K	198K	12.9M	83.5K
ChlorineConcentration	22.1M	880K	585K	20.8M	1.79K	176K	243K	15.5M	81.1K
Computers	2.81M	587K	195K	12.0M	1.19K	151K	180K	5.22M	52.1K
CricketX	4.43M	3.52M	2.34M	69.5M	1.65K	160K	255K	13.7M	120K
CricketY	4.43M	3.52M	2.34M	70.3M	1.39K	179K	260K	21.6M	140K
CricketZ	4.43M	3.52M	2.34M	61.4M	1.52K	148K	259K	13.1M	122K
Earthquakes	7.60M	572K	193K	17.8M	293	33.0K	234K	6.84M	25.2K
EOGHorizontalSignal	4.11M	3.52M	2.34M	49.6M	1.21K	209K	202K	11.5M	94.6K
EOGVerticalSignal	4.11M	3.52M	2.34M	38.7M	1.21K	147K	251K	13.8M	112K
EthanolLevel	10.3M	1.17M	780K	41.0M	933	149K	189K	7.96M	59.4K
FaceAll	6.42M	4.11M	2.73M	67.7M	1.28K	210K	267K	13.5M	109K
Fish	2.04M	2.11M	1.38M	15.5M	1.23K	176K	237K	11.9M	63.9K
FordA	172M	587K	195K	14.6M	183	18.6K	136K	15.3M	8.36K
FordB	42.6M	579K	194K	128M	1.15K	178K	265K	10.7M	69.9K
FreezerRegularTrain	4.36M	587K	195K	4.00M	238	35.0K	167K	13.5M	87.6K
GunPointAgeSpan	1.53M	594K	196K	1.57M	549	69.5K	169K	12.5M	39.8K
GunPointMaleVersusFemale	2.77M	594K	196K	4.08M	183	35.8K	171K	16.2M	19.9K
GunPointOldVersusYoung	2.22M	602K	198K	5.60M	183	24.3K	136K	17.0M	14.5K
Ham	2.18M	587K	195K	3.20M	769	108K	155K	8.99M	38.7K
HandOutlines	11.4M	579K	194K	67.1M	1.41K	189K	253K	9.59M	47.8K
Haptics	1.72M	1.47M	975K	12.5M	1.06K	116K	203K	15.3M	62.5K
InlineSkate	1.09M	2.05M	1.37M	11.5M	1.01K	145K	204K	18.3M	44.3K
InsectWingbeatSound	2.47M	3.23M	2.15M	28.8M	1.04K	154K	242K	12.0M	106K
LargeKitchenAppliances	4.26M	880K	585K	27.5M	1.12K	174K	234K	12.8M	75.6K
MixedShapesRegularTrain	10.2M	1.47M	975K	30.1M	1.28K	178K	213K	15.3M	67.5K
MixedShapesSmallTrain	4.69M	1.47M	975K	5.83M	659	90.0K	185K	11.0M	47.3K
NonInvasiveFetalECGThorax1	21.2M	12.3M	8.19M	206M	1.78K	181K	245K	18.3M	299K
NonInvasiveFetalECGThorax2	21.2M	12.3M	8.19M	146M	1.92K	147K	272K	20.4M	246K
OSULeaf	5.82M	1.76M	1.17M	15.1M	750	141K	176K	11.5M	62.4K
Plane	2.10M	2.05M	1.37M	7.38M	1.04K	86.4K	215K	12.6M	43.5K
PowerCons	2.31M	594K	196K	2.21M	512	55.4K	176K	8.88M	36.6K
RefrigerationDevices	4.35M	891K	589K	22.6M	1.15K	174K	239K	14.0M	74.6K
ScreenType	4.26M	880K	585K	37.0M	1.12K	143K	209K	9.44M	75.4K
SemgHandGenderCh2	3.39M	587K	195K	23.9M	1.02K	151K	196K	12.4M	58.8K
SemgHandMovementCh2	5.13M	1.76M	1.17M	59.9M	1.45K	177K	224K	22.7M	69.3K
SemgHandSubjectCh2	5.13M	1.47M	975K	45.3M	1.46K	201K	245K	21.4M	74.0K
ShapesAll	7.04M	17.8M	11.8M	82.4M	1.61K	191K	243K	19.5M	392K
SmallKitchenAppliances	4.26M	880K	585K	22.6M	787	142K	184K	6.33M	99.5K
StarLightCurves	11.6M	880K	585K	33.8M	439	153K	197K	10.2M	38.3K
Strawberry	12.5M	587K	195K	19.0M	1.23K	136K	258K	13.8M	54.2K
SwedishLeaf	5.72M	4.40M	2.93M	56.4M	1.43K	203K	259K	29.2M	144K
Trace	3.18M	1.14M	770K	5.54M	439	38.9K	145K	14.0M	30.2K
TwoPatterns	11.6M	1.17M	780K	56.3M	1.39K	154K	195K	11.6M	51.6K
UWaveGestureLibraryAll	34.5M	2.35M	1.56M	81.2M	1.37K	167K	264K	17.7M	74.9K
UWaveGestureLibraryX	10.4M	2.35M	1.56M	88.2M	1.61K	156K	241K	20.0M	98.2K
UWaveGestureLibraryY	14.4M	2.35M	1.56M	119M	1.39K	142K	217K	24.1M	124K
UWaveGestureLibraryZ	14.4M	2.35M	1.56M	64.5M	1.59K	167K	216K	22.7M	106K
Wafer	29.5M	587K	195K	12.4M	183	23.4K	136K	15.3M	6.70K
Worms	1.76M	1.47M	975K	13.6M	714	83.8K	175K	9.58M	31.9K
WormsTwoClass	2.41M	579K	194K	20.7M	769	112K	172K	14.1M	69.4K
Yoga	3.46M	594K	196K	18.5M	805	139K	214K	8.99M	49.9K

References

- [1] F. Petersen, C. Borgelt, H. Kuehne, and O. Deussen, “Deep differentiable logic gate networks,” in *Adv. Neural Inf. Process. Syst.*, vol. 35, 2022.
- [2] F. Petersen, H. Kuehne, C. Borgelt, J. Welzel, and S. Ermon, “Convolutional differentiable logic gate networks,” in *Adv. Neural Inf. Process. Syst.*, vol. 37, 2024.
- [3] C. Yue and N. K. Jha, “Learning interpretable differentiable logic networks,” *IEEE Trans. Circuits Syst. Artif. Intell.*, vol. 1, no. 1, pp. 69–82, 2024.
- [4] —, “Learning interpretable differentiable logic networks for tabular regression,” *arXiv preprint arXiv:2505.23615*, 2025.
- [5] C. H. Lubba, S. S. Sethi, P. Knaute, S. R. Schultz, B. D. Fulcher, and N. S. Jones, “catch22: CAnonical Time-series CHaracteristics: Selected through highly comparative time-series analysis,” *Data Min. Knowl. Discov.*, vol. 33, no. 6, pp. 1821–1852, 2019.
- [6] M. Christ, N. Braun, J. Neuffer, and A. W. Kempa-Liehr, “Time series feature extraction on basis of scalable hypothesis tests (tsfresh—a Python package),” *Neurocomputing*, vol. 307, pp. 72–77, 2018.
- [7] B. D. Fulcher and N. S. Jones, “hctsa: A computational framework for automated time-series phenotyping using massive feature extraction,” *Cell Syst.*, vol. 5, no. 5, pp. 527–531, 2017.
- [8] H. A. Dau, A. Bagnall, K. Kamgar, C.-C. M. Yeh, Y. Zhu, S. Gharghabi, C. A. Ratanamahatana, and E. Keogh, “The UCR time series archive,” *IEEE/CAA J. Autom. Sinica*, vol. 6, no. 6, pp. 1293–1305, 2019.
- [9] L. A. Zadeh, “Fuzzy sets as a basis for a theory of possibility,” *Fuzzy Sets Syst.*, vol. 1, no. 1, pp. 3–28, 1978.
- [10] K. Menger, “Statistical metrics,” *Selecta Math.*, vol. 2, pp. 433–435, 2003.
- [11] C. Rudin, “Stop explaining black box machine learning models for high stakes decisions and use interpretable models instead,” *Nat. Mach. Intell.*, vol. 1, no. 5, pp. 206–215, 2019.
- [12] M. T. Ribeiro, S. Singh, and C. Guestrin, ““Why should I trust you?” Explaining the predictions of any classifier,” in *Proc. ACM SIGKDD Int. Conf. Knowl. Discov. Data Min.*, 2016, pp. 1135–1144.
- [13] S. M. Lundberg and S.-I. Lee, “A unified approach to interpreting model predictions,” in *Adv. Neural Inf. Process. Syst.*, vol. 30, 2017.
- [14] R. Xin, C. Zhong, Z. Chen, T. Takagi, M. Seltzer, and C. Rudin, “Exploring the whole rashomon set of sparse decision trees,” in *Adv. Neural Inf. Process. Syst.*, vol. 35, 2022.
- [15] F. Wang and C. Rudin, “Falling rule lists,” in *Proc. Int. Conf. Artif. Intell. Stat.*, 2015, pp. 1013–1022.
- [16] C. Rudin, C. Chen, Z. Chen, H. Huang, L. Semenova, and C. Zhong, “Interpretable machine learning: Fundamental principles and 10 grand challenges,” *Stat. Surv.*, vol. 16, pp. 1–85, 2022.
- [17] Y. Umuroglu, Y. Akhauri, N. J. Fraser, and M. Blott, “LogicNets: Co-designed neural networks and circuits for extreme-throughput applications,” in *Proc. Int. Conf. Field-Program. Logic Appl.*, 2020, pp. 291–297.

- [18] A. Bagnall, H. A. Dau, J. Lines, M. Flynn, J. Large, A. Bostrom, P. Southam, and E. Keogh, “The UEA multivariate time series classification archive, 2018,” *arXiv preprint arXiv:1811.00075*, 2018.
- [19] M. Middlehurst, P. Schäfer, and A. Bagnall, “Bake off redux: A review and experimental evaluation of recent time series classification algorithms,” *Data Min. Knowl. Discov.*, vol. 38, no. 4, pp. 1958–2031, 2024.
- [20] T. Rakthanmanon, B. Campana, A. Mueen, G. Batista, B. Westover, Q. Zhu, J. Zakaria, and E. Keogh, “Addressing big data time series: Mining trillions of time series subsequences under dynamic time warping,” *ACM Trans. Knowl. Discov. Data*, vol. 7, no. 3, pp. 1–31, 2013.
- [21] M. Middlehurst and A. Bagnall, “The freshprince: A simple transformation based pipeline time series classifier,” in *Proc. Int. Conf. Pattern Recognit. Artif. Intell.* Springer, 2022, pp. 150–161.
- [22] A. Dempster, D. F. Schmidt, and G. I. Webb, “QUANT: A minimalist interval method for time series classification,” *Data Min. Knowl. Discov.*, vol. 38, no. 4, pp. 2377–2402, 2024.
- [23] J. Hills, J. Lines, E. Baranauskas, J. Mapp, and A. Bagnall, “Classification of time series by shapelet transformation,” *Data Min. Knowl. Discov.*, vol. 28, no. 4, pp. 851–881, 2014.
- [24] P. Schäfer, “The BOSS is concerned with time series classification in the presence of noise,” *Data Min. Knowl. Discov.*, vol. 29, no. 6, pp. 1505–1530, 2015.
- [25] P. Schäfer and M. Höggqvist, “SFA: A symbolic Fourier approximation and index for similarity search in high dimensional datasets,” in *Proc. 15th Int. Conf. Extend. Database Technol.*, 2012, pp. 516–527.
- [26] A. Dempster, D. F. Schmidt, and G. I. Webb, “MiniRocket: A very fast (almost) deterministic transform for time series classification,” in *Proc. 27th ACM SIGKDD Conf. Knowl. Discov. Data Min.*, 2021, pp. 248–257.
- [27] Z. Wang, W. Yan, and T. Oates, “Time series classification from scratch with deep neural networks: A strong baseline,” in *Proc. Int. Joint Conf. Neural Netw.*, 2017, pp. 1578–1585.
- [28] A. Ismail-Fawaz, M. Devanne, S. Berretti, J. Weber, and G. Forestier, “Lite: Light inception with boosting techniques for time series classification,” in *Proc. IEEE Int. Conf. Data Sci. Adv. Anal. (DSAA)*, 2023, pp. 1–10.
- [29] M. Middlehurst, J. Large, M. Flynn, J. Lines, A. Bostrom, and A. Bagnall, “HIVE-COTE 2.0: A new meta ensemble for time series classification,” *Mach. Learn.*, vol. 110, no. 11, pp. 3211–3243, 2021.
- [30] A. Guillaume, C. Vrain, and W. Elloumi, “Random dilated shapelet transform: A new approach for time series shapelets,” in *Proc. Int. Conf. Pattern Recognit. Artif. Intell.* Springer, 2022, pp. 653–664.
- [31] P. Schäfer and U. Leser, “WEASEL 2.0: A random dilated dictionary transform for fast, accurate and memory constrained time series classification,” *Mach. Learn.*, vol. 112, no. 12, pp. 4763–4788, 2023.
- [32] A. Dempster, F. Petitjean, and G. I. Webb, “ROCKET: Exceptionally fast and accurate time series classification using random convolutional kernels,” *Data Min. Knowl. Discov.*, vol. 34, no. 5, pp. 1454–1495, 2020.

- [33] A. Bagnall, J. Lines, J. Hills, and A. Bostrom, “Time-series classification with COTE: The collective of transformation-based ensembles,” *IEEE Trans. Knowl. Data Eng.*, vol. 27, no. 9, pp. 2522–2535, 2015.
- [34] C. W. Tan, A. Dempster, C. Bergmeir, and G. I. Webb, “MultiRocket: Multiple pooling operators and transformations for fast and effective time series classification,” *Data Min. Knowl. Discov.*, vol. 36, no. 5, pp. 1623–1646, 2022.
- [35] A. Meurer, C. P. Smith, M. Paprocki, O. Čertík, S. B. Kirpichev, M. Rocklin, A. Kumar, S. Ivanov, J. K. Moore, S. Singh, T. Rathnayake, S. Vig, B. E. Granger, R. P. Muller, F. Bonazzi, H. Gupta, S. Vats, F. Johansson, F. Pedregosa, M. J. Curry, A. R. Terrel, Š. Roučka, A. Saboo, I. Fernando, S. Kulal, R. Cimrman, and A. Scopatz, “SymPy: Symbolic computing in Python,” *PeerJ Comput. Sci.*, vol. 3, p. e103, Jan. 2017. [Online]. Available: <https://doi.org/10.7717/peerj-cs.103>
- [36] Y. Bengio, N. Léonard, and A. Courville, “Estimating or propagating gradients through stochastic neurons for conditional computation,” *arXiv preprint arXiv:1308.3432*, 2013.
- [37] H.-T. Cheng, L. Koc, J. Harmsen, T. Shaked, T. Chandra, H. Aradhye, G. Anderson, G. Corrado, W. Chai, M. Ispir *et al.*, “Wide & deep learning for recommender systems,” in *Proc. 1st Workshop Deep Learn. Recommender Syst.*, 2016.
- [38] T. Akiba, S. Sano, T. Yanase, T. Ohta, and M. Koyama, “Optuna: A next-generation hyperparameter optimization framework,” in *Proc. ACM SIGKDD Int. Conf. Knowl. Discov. Data Min.*, 2019, pp. 2623–2631.
- [39] F. Pedregosa, G. Varoquaux, A. Gramfort, V. Michel, B. Thirion, O. Grisel, M. Blondel, P. Prettenhofer, R. Weiss, V. Dubourg *et al.*, “Scikit-learn: Machine learning in Python,” *J. Mach. Learn. Res.*, vol. 12, pp. 2825–2830, 2011.
- [40] A. Paszke, S. Gross, F. Massa, A. Lerer, J. Bradbury, G. Chanan, T. Killeen, Z. Lin, N. Gimelshein, L. Antiga *et al.*, “Pytorch: An imperative style, high-performance deep learning library,” in *Adv. Neural Inf. Process. Syst.*, vol. 32, 2019.
- [41] M. Middlehurst, A. Ismail-Fawaz, A. Guillaume, C. Holder, D. Guijo-Rubio, G. Bulatova, L. Tsaprounis, L. Mentel, M. Walter, P. Schäfer, and A. Bagnall, “aeon: A python toolkit for learning from time series,” *J. Mach. Learn. Res.*, vol. 25, no. 289, pp. 1–10, 2024. [Online]. Available: <http://jmlr.org/papers/v25/23-1444.html>
- [42] P. Moritz, R. Nishihara, S. Wang, A. Tumanov, R. Liaw, E. Liang, M. Elibol, Z. Yang, W. Paul, M. I. Jordan *et al.*, “Ray: A distributed framework for emerging AI applications,” in *Proc. USENIX Symp. Oper. Syst. Des. Implement.*, 2018, pp. 561–577.
- [43] R. Liaw, E. Liang, R. Nishihara, P. Moritz, J. E. Gonzalez, and I. Stoica, “Tune: A research platform for distributed model selection and training,” *arXiv preprint arXiv:1807.05118*, 2018.